# The Geochemical News

Newsletter of The Geochemical Society

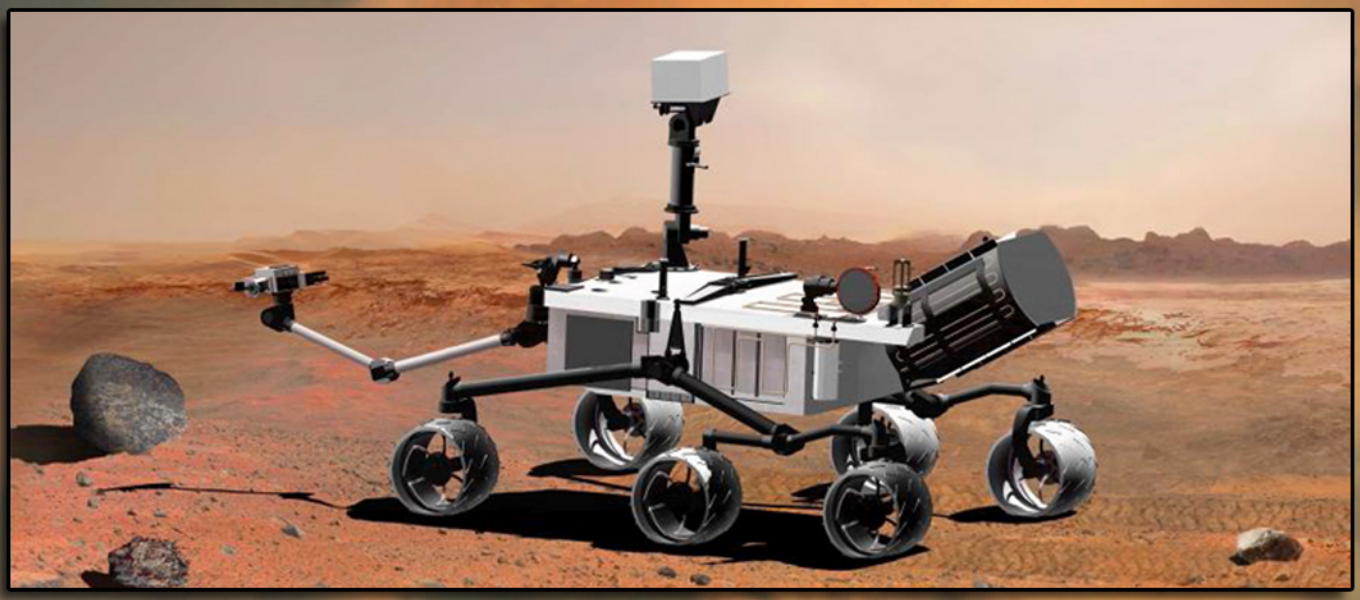

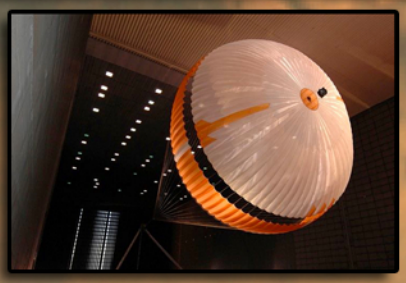

## Curiosity on Mars: Geochemical Instrumentation and Context Observations

Special Issue
Number 145
ISSN 0016-7010

# THE GEOCHEMICAL NEWS

Newsletter of The Geochemical Society

Issue 145 • June 2011

## *Curiosity* on Mars: Geochemical Instrumentation and Context Observations



Issue Editor: Paul Mahaffy
GN Editor: Stephen Komor
Web manager: Seth Davis

*The Geochemical News* (*GN*) is a publication of the Geochemical Society. It is distributed as a downloadable .pdf file as a benefit to members and is also available in HTML format on the Geochemical Society's website at: http://www.geochemsoc.org/publications/geochemicalnews/gn145jun11/


ISSN 0016-7010

The Geochemical Society
Washington University in St. Louis
Earth & Planetary Sciences
One Brookings Dr, CB 1169
Saint Louis, MO 63130-4899
gsoffice@geochemsoc.org
ph: 314-935-4131
fx: 314-935-4121
**www.geochemsoc.org**

# Sample analysis at Mars: Developing analytical tools to search for a habitable environment on the Red Planet

**Paul MAHAFFY**[a]
[a]NASA Goddard Space Flight Center Greenbelt, MD 20771, U.S.A.

Mars provides one of the most accessible locations in our solar system outside Earth into geological and geochemical windows through which to view planetary evolution from billions of years in the past until the present. Successful missions in the past decade to both study Mars from orbit and to land on its surface have dramatically advanced our understanding of our neighboring cold but volatile-rich planet. Taking advantage of nearly every recent launch window that presents itself every 2.135 years the 'follow the water' theme has been vigorously pursued as a first exploration step most relevant to the driving question of the possibility of past or present microbial life on Mars. With this exploration directive, the global distribution of near surface water ice and hydrated minerals was mapped from orbit by NASA's Odyssey spacecraft (Boynton et al., 2002) using measurements of the energy distribution of cosmic ray generated neutrons produced from the near surface. High latitude regions were inferred to be typically composed of more than 50% water ice in the top tens of centimeters of soil. Hard on the heels of this discovery, the Mars Exploration Rovers Spirit and Opportunity found convincing evidence at mid latitudes but on opposite sides of the planet of aqueous alteration by liquid water (Squyres et al., 2004 and 2008). This evidence came in the form of minerals (jarosite, goethite, and opaline silica) formed by aqueous transformation and also in the form of signatures of water flow revealed in returned images of cross-bedding in sedimentary layers from the rover cameras. The Phoenix high latitude lander mission (Smith et al., 2009) trenched down through surface soil to an icy layer and provided ground verification of the Odyssey measurement. More recent observations from high resolution orbiting telescopes and imaging spectrometers (Murchie et al., 2009) have resulted in a better understanding of the surface transformations over the history of Mars by water, giant impacts, volcanoes, winds, and the large scale movement of surface ice caused by the periodic variations in the planet's axial tilt (its obliquity). Rich assemblages of phyllosilicates (clays) and hydrated mineral layers continue to be revealed in many locations by imaging spectrometers on both the European Mars Express Mission and NASA's Mars Reconnaissance Orbiter. An emerging paradigm now paints a picture of an early wetter Mars that enabled clay formation in a more neutral chemical environment than the following more acidic sulfur dominated surface environment produced by immense volcanic activity (Bibring et al., 2006). Exposure of ancient terrains and the lack of plate tectonics for much of the history of Mars suggest that geochemical windows into the distant past may be preserved in the near-surface so that future surface landers and rovers may be able to explore the environmental conditions necessary for life in ancient sites.

The Mars Science Laboratory (MSL) now planned to be sent on its way to Mars in the 2011 launch opportunity is designed to explore habitability with a large heavily instrumented rover. After landing, MSL will be able to traverse 10's of kilometers over the 2-year mission lifetime (one Mars year) and access specific sites that have been identified from orbit by imaging and spectroscopy measurements. The MSL primary science goals are (1) to assess the past or present biological potential at the targeted site, (2) to characterize the site's geology at various spatial scales, and (3) to investigate other planetary processes that influence habitability. The MSL mission moving beyond the 'follow the water' theme seeks an even more detailed understanding of the history of the Mars environment (Grotzinger, 2009) and how significant transitions in this environment might have impacted potential habitats for even

**Figure 1.** An artist's conception of the MSL rover on the surface of Mars. MSL is able to carry a much more substantial payload to the surface of Mars than any other previous Mars lander.

**Figure 2.** The aeroshell that will protect the MSL lander during the first stages of the entry into the Mars atmosphere is shown in an environmental test chamber.

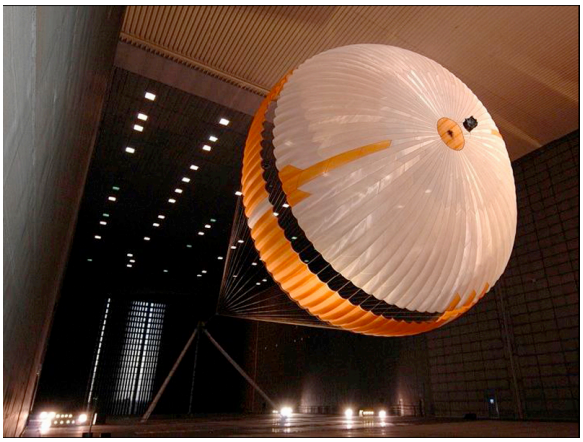

**Figure 3.** The parachute design that will be utilized during the descent is tested in a large wind tunnel.

the simplest microorganisms or even their chemical precursors.

Dust storms on Mars are predicted to enhance the abundance of hydrogen peroxide in the atmosphere to the point where it accumulates on the surface (Atreya et al., 2006). A first order question for MSL is whether organic compounds produced by early or current biological processes, by abiotic processes, or even delivered from space by meteoritic infall can be preserved in what is likely to be this oxidizing surface environment. MSL will not only search for these organic compounds but will also inventory other chemical building blocks of life containing carbon, hydrogen, nitrogen, oxygen, phosphorus, and sulfur compounds. Regardless of the fate of ancient or recent reduced carbon compounds in the Martian soils and rocks the chemical processes that might destroy or preserve organic compounds must be understood and so MSL intends to study the geology and chemistry in detail to interpret processes that have formed and transformed rocks and regolith. Planetary process that impact habitability such as climate change and loss of a portion of the atmosphere over time will be explored by MSL by signatures of these processes in isotopic composition, particularly in the inert noble gases in the atmosphere. MSL will be launched in late 2011 on an Atlas V 541 rocket. Its entry, descent, and landing (EDL) through the thin atmosphere of Mars in the late summer or fall of 2012 will utilize first a heat shield to slow down the entry vehicle during a guided descent, then deployment of a large supersonic parachute followed by a powered descent, and finally tethered release of the MSL rover directly onto its wheels from the descent stage hovering several meters above the surface. This final sky crane touchdown system is intended to enable a soft landing for the ~900 kg rover since airbag technology of the type used to protect the MER landers after their release from their parachute is not suitable for this size vehicle. The nominal mission duration is one Mars year (2 Earth years) although an additional exploration period may be realized in an extended MSL mission. Figure 1 shows an artist's conception of MSL on the surface of Mars and Figure 2 a picture of the MSL spacecraft and aeroshell being prepared for

| Table 1: Mars Science Laboratory Investigations | |
|---|---|
| **Remote Sensing Investigations Located on the MSL Mast** | |
| **Mastcam (PI, M. Malin):** High spatial resolution imaging and video to study geological features around the rover | **ChemCam (PI, R. Wiens):** Laser induced breakdown spectroscopy enables elemental analysis in the rover vicinity |
| **Contact Sensing Investigations Located on the Arm** | |
| **APXS (PI, R. Gellert):** Particle induced X-ray emission and fluorescence utilized to determine elemental composition of soils and rocks | **MAHLI (PI, K. Edgett):** Fine textures and structure of rocks and fines studied by securing microscopic images |
| **Environmental Investigations** | |
| **DAN (PI, I. Mitrofanov):** Hydrogen in water or hydrated minerals measured within one meter of the surface using a pulsed neutron generator and detector | **MARDI (PI, M. Malin):** High resolution imagery of the MSL landing site obtained during descent to provide context for the landed exploration |
| **RAD (PI, D. Hassler):** Radiation environment on the surface of Mars measured that could be a hazard to future human explorers. | **REMS (PI, J. Gómez-Elvira):** Winds, temperatures, pressure, and ultraviolet radiation measured with a suite of sensors located on the MSL mast. |
| **Analytical Laboratory Investigations** | |
| **CheMin (PI, D. Blake):** Mineralogy of powdered samples of rocks and soils established using X-ray diffraction and X-ray fluorescence | **SAM (PI, P. Mahaffy):** Chemical and isotopic composition of volatiles (including organics) established using a gas chromatograph mass spectrometer and a tunable laser spectrometer |

tests in a thermal vacuum chamber. Figure 3 is a picture of the massive parachute being tested in a large wind tunnel.

The MSL science payload summarized in Table 1 enables four different types of scientific investigation. Using the high resolution mast camera (Mastcam) and a laserinduced breakdown spectrometer (LIBS or ChemCam) the geology and a rapid survey of chemical differences in targeted rocks in the immediate vicinity of the rover can be established. At the same time the neutron detector (DAN) provides information on the near subsurface abundance of water containing minerals. Once these tools identify an interesting site and specific rocks or soils the MSL arm is extended to allow a more detailed examination by a microscope (MAHLI) and an alpha particle X-ray spectrometer (APXS) that can establish elemental composition. Finally, samples of greatest interest are processed into powder by a rotary percussive drill/sieve system and delivered to two instruments in the interior of the rover. In these instruments the mineralogy of the sample can be established by an X-ray diffraction/X-ray fluorescence instrument (ChemMin) and the search for organics, inorganic volatiles, and the measurement of various isotopes will be carried out by a suite of instruments (SAM). The SAM science investigation, its instruments, and supporting technology is described in more detail below. Finally, atmospheric winds, temperatures, pressures, and ultra violet radiation are measured by an additional instrument in the mast (REMS), the energetic radiation environment of the type that could be hazardous to future human explorers is measured with the RAD instrument, and the geological context of the landing site is obtained by the descent camera MARDI.

The diversity of geology and mineralogy revealed by ongoing orbital tools provides an

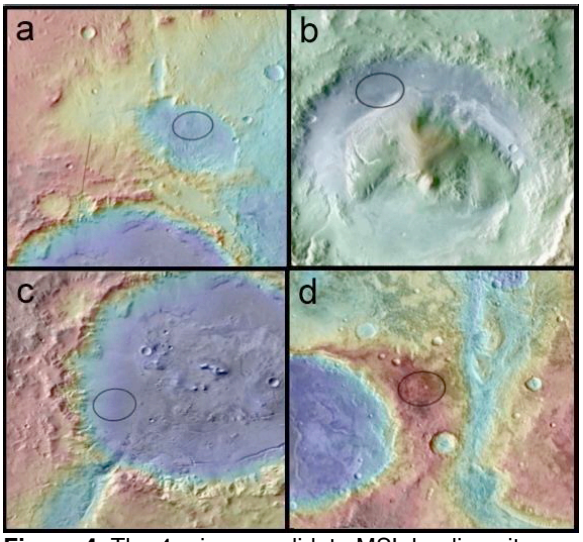


**Figure 4.** The 4 prime candidate MSL landing sites are shown with the color in these orbital images showing elevation. The sites are (a) Eberswalde Crater, (b) Gale Crater, (c) Holden Crater, and (d) Mawrth Valles. Landing ellipses of approximately 20 km are shown that avoid areas of high slopes or areas cluttered with large rocks.

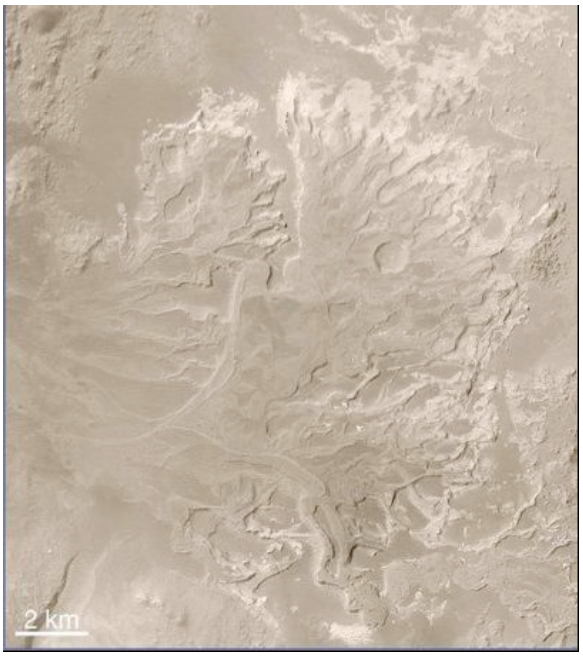


**Figure 5.** The Eberswalde delta features are clearly evident in this image from space (Image: Malin Space Sciences/NASA/JPL).

excellent set of tools to select a MSL landing site that can best address the mission's scientific goals. Several dozen proposed landing sites have been presently narrowed down to four through a series of open workshops that brought Mars scientists and MSL engineers together to discuss the relative merits of each site. In parallel with the development of the scientific motivation for landing at particular site, the practical issue of avoiding rocky terrains and extreme slopes was addressed and the altitude and winds at the landing site considered. Landing more than 1 km above the mean Mars altitude, for example, might not give the MSL entry system enough time in the atmosphere to robustly exercise its multiple deceleration modes so lower altitude sites are preferred. Fortunately, the four sites that were judged to be of extraordinary scientific interest appear to also provide the required safety factors for the MSL entry, descent, and landing (EDL) systems. Listed from North to South these are Mawrth Vallis, Gale Crater, Eberswalde Crater, and Holden Crater. Orbital images of these sites superimposed on a color coded map of altitude from the Mars Orbiter Laser Altimeter are shown in Figure 4 together with candidate landing ellipses that avoid much of the rocky or highly slopped terrain.

Two of the landing sites show clear evidence of the past presence of flowing water (Malin and Edgett, 2003). A well-defined delta (Figure 5) is present inside the Eberswalde Crater that could be reached through a rover traverse. Likewise, a reasonable explanation for features observed at the Holden Crater candidate-landing site is that ancient sedimentary deposits from a lake that formed in the crater were later exposed by a river that spilled over the walls of the crater from the south. The sediments in both these locations are compelling locations for the exploration of habitability with the MSL. Compelling spectroscopic features are among the factors that provide strong motivation for the in situ exploration of the Gale Crater and Mawrth Vallis candidate landing sites. A rich sequence of layered terrain with diverse spectroscopic signatures includes both clays and sulfates in the central mound of Gale crater (Figure 6). Slopes are gentle enough in some locations that these

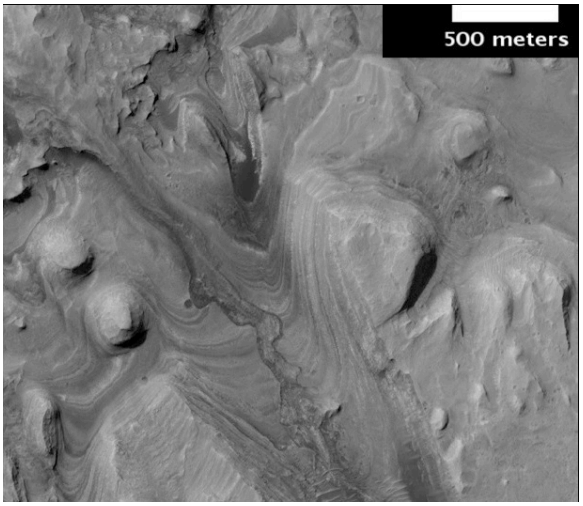


**Figure 6.** Gale crater shows multiple layers in this high resolution image from the Mars Reconnaissance Orbiter (Image: NASA/JPL/University of Arizona).

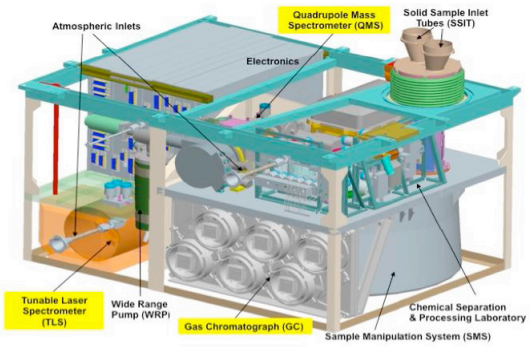


**Figure 7.** A three dimensional model of SAM shows the instruments and major subsystems.

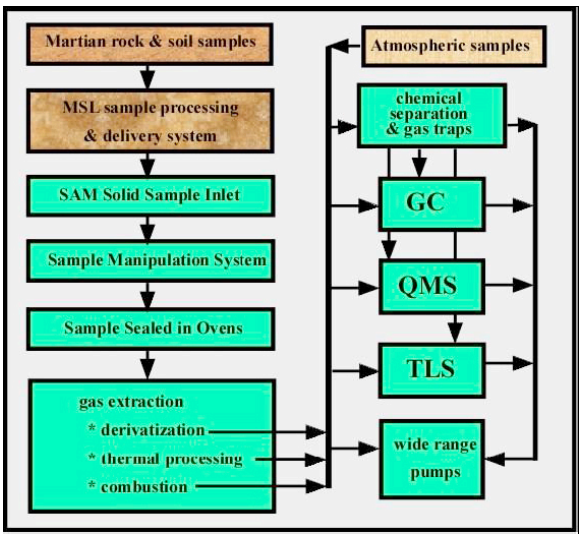


**Figure 8.** The SAM sample processing flow is illustrated for both transfer of solid and gaseous samples.

**Figure 9.** The SAM suite is here being prepared for tests in its environmental chamber that span the range of temperatures and pressures that SAM will encounter on the surface of Mars.

sites can be reached by an extended traverse from the smoother landing site. Mawrth Vallis shows some of the strongest and most diverse phyllosilicate signatures seen anywhere on the planet. This site is evidently from the early Noachian period of Mars with the spectral features more recently exposed by erosion processes. An attractive feature of the Mawrth Vallis site is that features of interest are found in the landing ellipse and can be accessed without a long traverse.

A 3 dimensional representation of the SAM suite of instruments and associated supporting subsystems is shown in Figure 7. The three instruments that measure either atmospheric gas or gas extracted from solid samples are a quadrupole mass spectrometer (QMS), a tunable laser spectrometer (TLS), and a gas chromatograph (GC). The six column GC not only has its own detectors, but also can operate together with the QMS as a gas chromatograph mass spectrometer (GCMS). The supporting systems are a Chemical Separation and Processing Laboratory (CSPL) and sample manipulation system (SMS). The manipulation of solid sample and the processing of gaseous samples in SAM is schematically illustrated in the block diagram of Figure 8. The SAM suite has been tested in an environmental chamber designed specifically for this instrument (Figure 9) where the temperatures and pressures

encountered by the instrument can be set to those expected inside the rover on the surface of Mars.

The Mars atmosphere is sampled by SAM micro-valve operations that introduce a small volume of atmospheric gas through an inlet tube to the SAM instruments. This manifold gas volume is either introduced into the QMS through a capillary leak or directed to the TLS. Finely sieved solid phase materials delivered from the MSL rotary percussive drill to a SAM inlet funnel that delivers sample down a tube to one of 74 SAM sample cups. The funnel is vibrated during sample delivery to insure complete transfer to the cup. The cup is then inserted into a SAM oven and thermally processed to release volatiles. The gas processing manifold includes high conductance and micro valves, chemical and mechanical pumps, carrier gas reservoirs and pressure regulators, pressure monitors, the pyrolysis ovens, the chemical scrubbers and getters, and all the associated heaters and temperature sensors.

The quadrupole mass spectrometer can operate in static or dynamic mode with a mass range of 2-550 m/z. Its ion detector dynamic range $>10^{10}$ with both a channeltron pulse counting electron multiplier and a Faraday Cup. The crosstalk between adjacent peaks is greater than one million which enables isotopes of interest to be accurately measured. The gas chromatograph utilizes on of six columns to separate a complex mixtures of organic compounds into its molecular components which are detected both by the mass spectrometer and the thermal conductivity detectors on 5 of the 6 columns. The GCMS detection limit exceeds the part per billion mission requirement for organic detection. The TLS is a two channel Herriott cell design spectrometer that provides detection of $CH_4$, $H_2O$, and $CO_2$ and the isotope ratios $^{13}C/^{12}C$, $^{18}O/^{16}O$, and $^{17}O/^{16}O$ in carbon dioxide, D/H in water, and $^{13}C/^{12}C$ in methane. The TLS sensitivity for atmospheric gas is < 1 ppb and the detection limit can be substantially reduced by methane enrichment in SAM's CSPL.
A mixture of several calibration gases is brought to Mars in SAM to be used at regular intervals during the mission. The calibration gas cell includes $N_2$, $CO_2$, Ar, and a Xe mix that is heavily spiked with $^{129}X$ to clearly distinguish it from terrestrial or martian xenon. Three fluorocarbon compounds are included in this cell to evaluate the performance of the GCMS before launch and over the course of the mission. An organic check material that processes the same fluorocarbons adsorbed on an inert silica glass matrix through the entire sample processing chain provides both a check on the performance of the SAM organics detection and the cleanliness of the sample transfer chain.

The first steps by the SAM suite to search for organics will be to heat a powdered sample of rock and analyze the evolved gas. This analysis is first implemented with rapid mass spectrometer scans as the sample is heated and a portion of the gas stream introduced through capillary leaks into the QMS. Subsequently a GCMS analysis of gas trapped from the evolved gas stream is carried out to enable a complex mix of organics, if present, to be separated into their individual constituents. The study of the source of organics will rely first of all on an examination of patterns such as molecular weight distribution, linearity or branched characteristics of hydrocarbons, and odd/even enhancements in chain length. Terrestrial biology leaves what are often such distinct patterns while extraction of carbon compounds from meteorites shows us that hydrocarbons produced and processed by abiotic processes in space exhibit more extensive branching and more randomized chemical structures. A second tool available to SAM for organics analysis will be carbon isotopic analysis. Refractory organics can be combusted to $CO_2$ and their carbon and oxygen isotopes measured by the TLS. Comparisons of $^{13}C/^{12}C$, for example, can then be made with these ratios in meteoritic carbon and with the isotopic composition of the oxidized carbon in the atmosphere.

Finally if a site rich in organics is identified samples can be analyzed in SAM utilizing one of the several chemical derivatization cells. In this experiment the foil sealing a metal cup is punctured and sample introduced to a liquid consisting of a mixture of the solvent DMF (dimethylformanide) and a derivatization agent MTBSTFA (N,N-Methyl-tert,-

butl(dimethylsily)trifluoroacetamide). The silylation reaction that ensues turns polar molecules such as carboxylic acids and amino acids into non-polar volatile compounds that readily make their way through the GC column into the QMS. This extraction method has been utilized in our laboratory to analyze organics from samples of the highly oxidized, organic-poor soil from the driest part of the Atacama desert. This wet extraction method avoids the potential issues associated with the transformation by oxdation of these organic compounds during pyrolysis.

Localized methane has recently been identified by spectroscopy in the atmosphere of Mars (Formisano et al., 2004; Krasnopolsky et al., 2005; Mumma et al., 2009). What is just as exciting as the discovery itself is the observation of its rapid disappearance over a period of weeks or months (Mumma et al., 2009). The lifetime of methane in the Mars atmosphere is predicted to be more than 300 years and there is evidently a destruction mechanism that operates on a much faster timescale (Lefevre and Forget, 2009). The SAM TLS undertakes a sensitive search for atmospheric methane and its $^{13}C$ isotope. Methane will also be enriched for the TLS measurements in the SAM gas processing system to improve the precision of the isotope measurement. Regular measurements over the course of the two-year landed mission will provide better temporal resolution than the presently sparse ground-based measurements. As extensive terrestrial field work has illustrated (Sherwood Lollar et al., 2006), a broad range of measurements will ultimately be required to definitively prove if the source of methane on Mars is biotic or produced abiotically by processes such as serpentization. Related experiments carried out by SAM that we expect will contribute to the study of the source of the methane are measurements of the mixing ratio of other trace hydrocarbons and isotope ratios such as D/H in water. These measurements will include atmospheric samples and gases released from surface rock and soil samples.

Regardless of outcome of the MSL/SAM search for organics, the SAM suite is expected to provide a wealth of data on the chemical and isotopic composition of the atmosphere and of volatiles in solid samples. Measurements of the SNC (Martian) meteorites combined with the 1976 Viking lander data indicate that D/H, $^{15}N/^{14}N$, and $^{38}Ar/^{36}Ar$ are all fractionated and enriched in the heavier isotopes. A precise measurement of the major Xe isotopes could solidify the widely held belief that Mars is really the origin of the SNC meteorites. Assuming this is found to be the case, a better precision SAM measurement of atmospheric isotope ratios of the other noble gases and $^{15}N/^{14}N$ in nitrogen could help determine what portion of the SNC gas was trapped from the atmosphere during the impact melt event or represents components present in the solid when these fragments were ejected into space. Although the present Mars atmosphere is being removed by processes such as solar wind sputtering, photo dissociation, and dissociative recombination of species such as $N_2^+$ with electrons it is not yet clear what the Mars composition and atmospheric pressure was more than 3.5 billion years ago when liquid water was probably much more prevalent and left its mark in the features seen in Eberswalde and Holden craters. Better measurements of carbon, nitrogen, hydrogen, oxygen, and noble gas isotopes with SAM will provide improved constraints on models of atmospheric loss over the history of the planet. If MSL lands on ancient terrain a comparison of these light isotopes in ancient rocks compared with the present atmosphere will give additional constrains on these models of atmospheric evolution.

MSL has the range of analytical tools to search for windows that could preserve evidence of the nature of ancient environments. Exploration at the MSL landing site is not limited to the search for organic compounds, but is planned as a systematic in situ examination of geomorphology, microscopy, mineralogy, chemistry, and isotopes over an extended area on the surface of Mars where hypotheses regarding habitability and geological processes can be tested with multiple experiments in diverse locations. The in situ studies will be well supported by orbital imaging and spectroscopic data. We anticipate that the MSL investigations will provide a significant step forward in exploring the processes that have shaped Mars

and in our understanding of the present or past biological potential of the selected landing environment.

## REFERENCES

Atreya, S.A. et al., (2006), Oxidant Enhancement in Martian Dust Devils and Storms: Implications for Life and Habitability, Astrobiology 6, 439-450.

Bibring, J.-P., et al. (2006), Global mineralogical and aqueous Mars history derived from OMEGA/Mars Express data, Science, 312, 400 - 404, doi:10.1126/science.1122659.

Boynton, W.V. et al. (2002), Distribution of Hydrogen in the Near-Surface of Mars: Evidence for Subsurface Ice Deposits, Science Express 10.1126, 1073722.

Formisano V. et al. (2004), Detection of methane in the atmosphere of Mars, Science 306, 1758-1761.

Grotzinger, J. (2009), Beyond water on Mars, Nature Geoscience 2, 1-3.

Krasnopolsky V. A., et al., (2005) Detection of methane in the martian atmosphere: Evidence for life?; Icarus, 172, 537-547.

Lefevre, F. and Forget, F. (2009), Observed variations of methane on Mars unexplained by known atmospheric chemistry and physics, Nature 460, 720-723.

Malin, M.C. and Edgett, K.S. (2003), Evidence for persistent flow and aqueous sedimentation on early Mars, Science, 302, 1931-1934.

Mumma M. J. et al. (2009), Strong release of methane on Mars in northern summer 2003, Science, 323, 1041-1045.

Murchie, S.L. et al. (2009), A synthesis of Martian aqueous mineralogy after 1 Mars year of observations from the Mars Reconnaissance Orbiter, Journal of Geophysical Research, 114, E00D06, doi:10.1029/2009JE003342.

Sherwood Lollar, B. (2006), Unravelling abiogenic and biogenic sources of methane in the Earth's deep subsurface, Chemical Geology 226, 328-339.

Smith, P. (2009), H2O at the Phoenix landing site, Science 325, 58-61.

Squyres, S.W. et al. (2008) Detection of silica-rich deposits on Mars. Science 320, 1063-1067.

Squyres, S.W. and 49 CoAuthors (2004), The Opportunity Rover's Athena Science Investigation at Meridiani Planum, Mars, Science 306, 1698-1703.

**Introduction by Paul Mahaffy (NASA Goddard Space Flight Center)**

The past decade of Mars missions has been a golden age of Mars exploration with a focus on the habitability of our next-door neighbor planet. With every new set of successful measurements from surface rovers or from orbit a fresh and often surprising perspective emerges on the geological and geochemical processes that brought Mars to its present cold and dry state. In the first contribution of this series (Geochemical News 141) we surveyed the recent progress from several such missions and examined the measurements we hope to make from instruments on a highly sophisticated rover (Curiosity) to be launched in 2011. With the present contribution, Bethany Ehlmann, one of the recent leaders in analyzing and interpreting Mars orbital infrared spectroscopy data will describe these techniques and results and the new view of the history of Mars that is emerging from these studies. (See NASA's illuminating animation at http://mars.jpl.nasa.gov/mro/gallery/video/)

# Diverse aqueous environments during Mars' first billion years: the emerging view from orbital visible-near infrared spectroscopy

**Bethany EHLMANN**[a*]

[a] Universite Paris-Sud, Institut d'Astrophysique Spatial, Bat 121, FR-91405 Orsay Cedex FRANCE
(formerly Brown University)

* Email: bethanyehlmann@gmail.com

Phyllosilicates, sulfates, carbonates, zeolites, chlorides, perchlorates, and opaline silica: news of discoveries on Mars is starting to read like a mineralogy textbook. With the arrival of orbiting visible/near-infrared (VNIR) spectrometers, first in 2003 on the European Space Agency's Mars Express followed in 2006 by NASA's Mars Reconnaissance Orbiter (MRO), it is now clear that chemical and mineralogic evidence of past aqueous geochemical processes persists to the present, recorded in rocks and sediments. Coupled with data from landed missions, Mars exploration is moving beyond excitement about simply past liquid water towards understanding that ancient Mars probably hosted a diverse array of aqueous environments. Recent data suggest that hydrothermal, lacustrine, and pedogenic settings were part of the Martian landscape during its first billion years. Could one (or more) of these environments have been habitable or inhabited? Using the current data to guide the upcoming set of landed and orbital missions, we may be poised to find out. Here I review recent mineralogic findings, detail the methods, and discuss implications for understanding the first billion years of Mars history-a period in which the geologic record on Earth is sorely lacking.

## FOLLOWING THE WATER...AND THE MINERALS

For the past decade, "follow the water" has been NASA's guiding principle for selection of Mars exploration missions and landing sites. The reason is simple: on Earth wherever we find water we find life. Tracing the history of this important Mars volatile may be our best means of understanding whether life could have existed there, as well as understanding the fundamental processes necessary to sustain water-rich worlds like our own through time.

Since the Mariner missions of the late 1960s, it has been known that liquid water was once a powerful force shaping Mars' surface. Since the first Mariner and Viking orbiters,

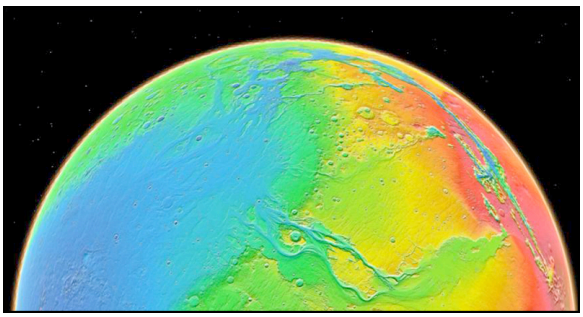

**FIGURE 1.** Topographic map showing large outflow channels and valleys draining into Mars' northern lowlands. In spite of abundant morphologic evidence

for liquid water, until recently orbiting spectrometers, orbital imaging has revealed large outflow channels, valley networks, evidence for crater lakes and, some posited, a possible northern ocean (Figure 1). Yet subsequent missions did not reveal the mineralogy and chemistry one might expect for a once watery world. Elemental composition measurements from landers and rovers showed rocks of primary volcanic composition. A few tantalizing hints of salts in Mars soils and in Mars meteorites pointed to at least small amounts of liquid water, but the basaltic rocks had not altered to clays or oxides. There appeared to be no secondary rocks, e.g. carbonates, that on Earth precipitate in large bodies of water and that should precipitate on Mars from waters in equilibrium with its 95% CO2 atmosphere.

no large deposits of altered minerals had been found.

But in 2004, following the water took an exciting, chemical/mineralogical turn. The Opportunity Mars Exploration Rover discovered sulfate-rich sedimentary rocks at Meridiani Planum, most likely deposited in shallow surface waters (Squyres et al., 2004). Then the Observatoire pour l'Minéralogie l'Eau les Glaces et l'Activité (OMEGA) visible/near-infrared imaging spectrometer on Mars Express began finding hydrated minerals from orbit (Bibring et al., 2005; for methods, see 'Identifying minerals from orbit' below). One class was the sulfate salts, such as at Meridiani, found in rocks from Mars' middle epoch, the Hesperian, approximately 2.9-3.7 Gyr. The second class was phyllosilicates, in this case Al-, Fe-, and Mg- smectite clays, found in the most ancient Noachian rocks, >3.7 Gyr. The youngest

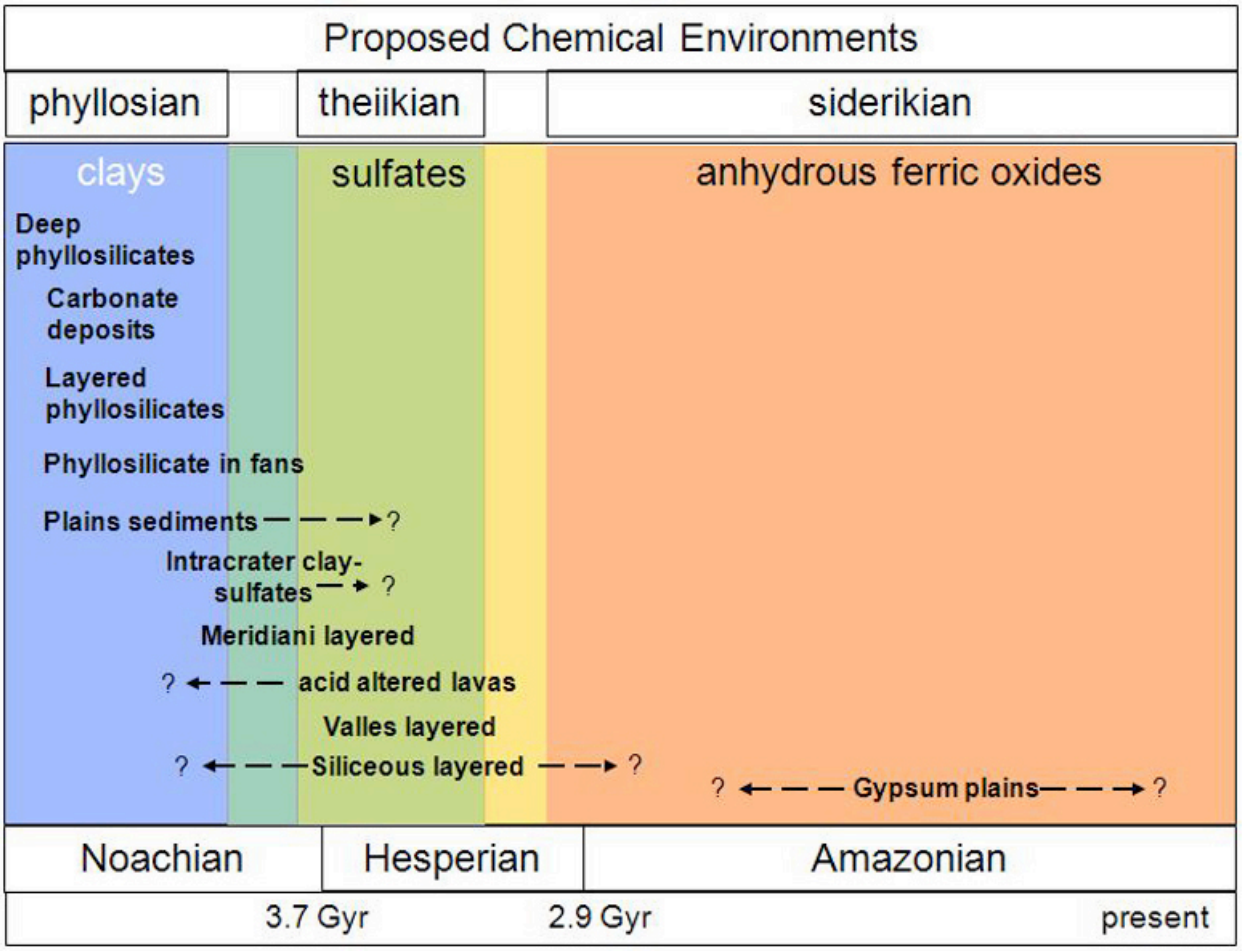

**FIGURE 2.** Chemical environments on Mars, adapted from Murchie et al., 2009 with mineralogic epochs from Bibring et al., 2006. The age dates for the Mars epoch boundaries are from Hartmann & Neukum (2001) cratering chronology.

**Table 1.** Minerals resulting from aqueous alteration, discovered on Mars through January 2010. All mineral phases are observed from orbit with VNIR spectroscopy except for phases in italics, which have been reported by other orbiting and landed missions.

| Class | Group/mineral | Formula | References |
|---|---|---|---|
| Phyllosilicates | Fe/Mg smectites (e.g., nontronite, saponite) | $(Ca, Na)_{0.3-0.5}(Fe,Mg, Al)_{2-3}(Si, Al)_4O_{10}(OH)_2$ | Poulet et al., 2005; Mustard et al., 2008 |
| | Montmorillonite | $(Na,Ca)_{0.33}(Al,Mg)_2(Si_4O_{10})(OH)_2$ | Poulet et al., 2005; Mustard et al., 2008 |
| | Kaolin group minerals (e.g. kaolinite, halloysite) | $Al_2Si_2O_5(OH)_4$ | Bishop et al., 2008; Ehlmann et al., 2009 |
| | Chlorite | $(Mg,Fe^{2+})_5Al(Si_3Al)O_{10}(OH)_8$ | Mustard et al., 2008; Ehlmann et al., 2009 |
| | Serpentine | $(Mg, Fe)_3Si_2O_5(OH)_4$ | Ehlmann et al., 2009 |
| | High charge Al,K phyllosilicate (e.g. muscovite or illite) | $KAl_2AlSi_3O_{10}(OH)_2$ | Mustard et al., 2008; Ehlmann et al., 2009 |
| **Other hydrated silicates** | Prehnite | $Ca_2Al(AlSi_3O_{10})(OH)_2$ | Clark et al, 2008; Ehlmann et al, 2009 |
| | Analcime | $NaAlSi_2O_6 \cdot H_2O$ | Ehlmann et al., 2009 |
| | Opaline silica | $SiO_2 \cdot H_2O$ | Milliken et al., 2008; Ehlmann et al., 2009 |
| **Carbonates** | Magnesium carbonate (e.g. magnesite) | $MgCO_3$ | Ehlmann et al., 2008b |
| | *Calcium carbonate* | *$CaCO_3$* | *Phoenix lander (Boynton et al., 2009)* |
| **Sulfates** | Fe/Mg mono- and poly-hydrated sulfates | $(Fe,Mg)SO_4 \cdot nH_2O$ | Gendrin et al., 2005 |
| | Gypsum | $CaSO_4 \cdot 2H_2O$ | Langevin et al., 2005 |
| | Alunite | $KAl_3(SO_4)_2(OH)_6$ | Swayze et al., 2008 |
| | Jarosite | $KFe^{(III)}_3(OH)_6(SO_4)_2$ | Milliken et al., 2008 |
| | not a named mineral | $FeSO_4(OH)$ | Swayze et al., pers. comm. |
| **Chlorides** | *chlorides* | *metalCl* | *Thermal Emission Spectrometer (Osterloo et al., 2008)* |
| **Perchlorates** | *perchlorates* | *$(Mg,Ca)(ClO_4)_2$* | *Phoenix Lander (Hecht et al., 2009)* |
| **Fe Oxides** | Hematite | $Fe_2O_3$ | Christensen et al., 2000; Bibring et al., 2007 |
| | Goethite | $FeO(OH)$ | Farrand et al., 2009 |

Amazonian terrains, <2.9 Gyr, had none of these hydrated minerals. This suggested a directional evolution for Mars, traceable through mineralogy (Bibring et al., 2006). A wet, circum-neutral pH clay-forming epoch ("phyllosian") was followed by a drier, more acidic sulfate-forming epoch ("theiikian"). By three billion years ago, only anhydrous alteration processes persisted over large scales ("siderikian").

The higher spatial and spectral resolution NASA follow-on to OMEGA, the Compact Reconnaissance Imaging spectrometer for Mars (CRISM; Murchie et al., 2007) on MRO has discovered many more occurrences of hydrated minerals than previously known as well as refined the detections of phyllosilicates and sulfates to reveal extraordinary mineralogic diversity within these classes as well as new mineral classes (Table 1). It is now possible to perform meters-scale geologic mapping from Mars orbit that includes both morphological and mineralogical properties of the units. By understanding the context and associations of these diverse alteration minerals, we are better able to distinguish the geological environment in which they formed. Coupled mineralogy with morphology allowed the identification of distinct chemical environments and their rough time ordering (Figure 2; Murchie et al., 2009), which we detail further below (‘Mineralogic clues to the first billion years').

## IDENTIFYING MINERALS FROM ORBIT

The fundamental advance that led to the discovery of these diverse water-related minerals only recently has been the application of orbital hyperspectral, visible/near-infrared (VNIR) imaging. The 0.4-2.6 μm wavelength region has proven to be most useful for mineral identification on Mars. VNIR spectroscopy is a technique commonly employed in the laboratory that is sensitive to changes in the energy state of transition metals' outer electrons (Fe is especially important in rock-forming minerals) as well as vibrations between atoms chemically bonded in mineral structures. The electrons and vibrating molecules, respectively, absorb radiation at characteristic wavelengths leading to distinctive absorption features in reflected light spectra that are often diagnostic of specific minerals. Usually, the electronic transition absorptions are broad and occur at wavelengths <1.5 μm (Burns, 1993). The fundamental vibrations due to OH, CO3, and H2O occur at much longer wavelengths (3-15 μm), but overtones and combination tones occur in the VNIR range measured by orbiting instruments. While these are weaker than the fundamentals in transmission spectra, light at VNIR wavelengths is multiply scattered in particulate media on planetary surfaces. The result is that the overtones and combinations may sometimes be stronger than the fundamentals that occur in the thermal infrared wavelengths (Clark et al., 1990).

The imaging spectrometers collect light in two different ways. In its infrared channels, OMEGA is a whisk broom imager which scans back and forth across the surface as it passes over, collecting one pixel in 352 wavelengths (0.35-5.1 μm) at a time with a spectral sampling of 7-20nm. CRISM is a push broom imaging spectrometer which collects a single row of pixels in 544 wavelengths (0.4-4.0 μm). Both instruments build up an image, north-south or south-north along the path of their polar orbits. The end result for each observation is the same: an image cube with x and y spatial dimensions and a z spectral dimension so that the VNIR spectrum of each pixel on the surface can be interrogated separately. OMEGA's spatial resolution ranges from 300-4800m/pixel, and global coverage is nearly complete. CRISM will complete a global map of Mars at 200m/pixel and in targeted mode acquires images at up to 18m/pixel.

The raw sensor data are corrected to radiance using laboratory data and data from an onboard calibration sphere. They are then converted to illumination angle-corrected I/F, an effective reflectance, by ratioing to the solar spectrum at Mars distance and dividing by the cosine of the incidence angle of light. To investigate surface mineralogy it is necessary to correct for strong bands resulting from atmospheric absorptions. Although more

complex methods exist, most commonly employed is the "volcano scan method" in which each pixel is divided by scaling an atmospheric transmission spectrum to fit the band depth of the CO2 triplet absorption at 2.0 μm. The atmospheric transmission spectrum used is derived by taking observations over the base and top of the 27-km high Olympus Mons volcano and ratioing the difference. Commonly, corrected data from an area of interest on the surface are also ratioed to corrected data from a "boring" area to eliminate residual artifacts from instrument calibration and highlight the distinctive absorption features.

After these corrections are made, individual spectra or spectra averaged over a given region can then be compared to laboratory spectra (e.g. Clark et al., 2007; http://speclab.cr.usgs.gov/spectral.lib06/) to make mineral identifications (Figure 3 and 4). For example, in smectites, the principal absorptions are near 1.4, 1.9 and 2.2-2.3 μm. These are due to vibrations of water and OH, water, and metal-OH structural elements, respectively. Shifts in band position occur, however, when Fe- (1.43, 2.29) vs. Mg- (1.39, 2.32) vs. Al- (1.41, 2.21) is the principal octahedral cation, allowing even structurally similar phases such as nontronite, saponite, and montmorillonite to be distinguished from orbit (Clark et al., 1990; Mustard et al., 2008).

Once identified, by mapping absorption band depth (Pelkey et al., 2007) or using more sophisticated parameters to examine overall spectral shape (Clark et al., 2003), the distribution of VNIR spectral signatures diagnostic of particular minerals can be mapped spatially. The high-resolution mineralogic data can then be combined with high-resolution imaging data sets-down to 25 cm/pixel resolution with MRO's HiRISE camera-to study mineralogy in concert with morphology.

## MINERALOGIC CLUES TO THE FIRST BILLION YEARS

As Figure 2 shows, nearly a dozen new aqueous chemical environments have been identified on Mars and are now the ongoing

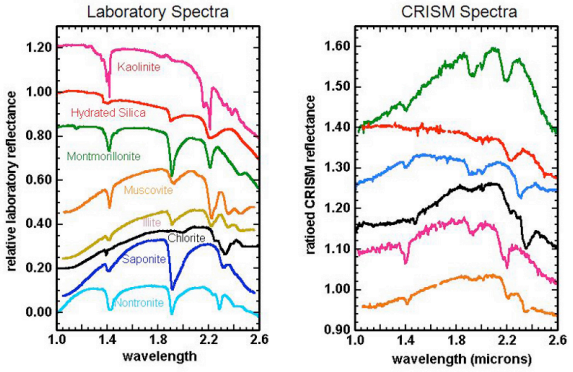


**FIGURE 3.** Selected hydrated silicate minerals discovered by CRISM (Mustard et al., 2008; Bishop et al., 2008; Ehlmann et al., 2009). Spectra have been colored so as to match CRISM spectral data to the most probable mineralogic match, based on examination of laboratory spectra. In some cases, mineral identifications cannot be made uniquely (e.g. muscovite vs. illite, orange/yellow) or phases on Mars are intermediate between endmember minerals with solid solution series (e.g. Fe/Mg smectite with composition between nontronite and saponite endmembers, blue/cyan)

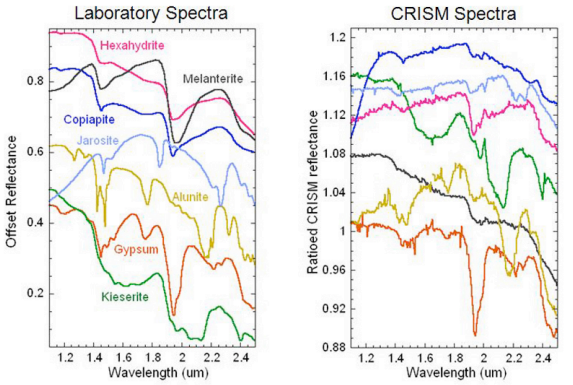


**FIGURE 4.** Selected sulfate minerals discovered by CRISM (Swayze et al., 2008; Murchie et al., 2009; Roach et al., 2009)

subject of intensive study (Murchie et al., 2009). A period of particular interest is the Noachian and the Noachian to Hesperian transition. During this period of Earth's history many important events happened: the first crust formation, the first liquid water, late heavy bombardment by meteorites, prebiotic chemistry and events leading to the origin of life. When did the Earth become habitable and when did it become inhabited? The timing and environmental conditions remain shrouded in

mystery due to the recycling of the rock record by plate tectonics. Far less than 1% of Earth's rock record is from this period and much of what does exist has been heavily altered by metamorphism, weathering, and more recent biologic activity. However, about half of Mars' crust dates back to before 3.5 Gyr. Moreover, this appears to be the period where liquid water played the greatest role in planetary geologic processes. Little is known about these early conditions and a big question is why did Mars apparently begin to dry by the end of its first billion years. By studying the environments of early Mars, we gain insight into the history of water on Mars and also the earliest watery environments on terrestrial planets.

## ENVIRONMENTAL HISOTRY FROM MINERALOGY

While some of the minerals on Mars form under a variety of geochemical conditions and at relatively unconstrained temperatures and pressures (e.g. smectites, chlorites, gypsum), some of the minerals form in only narrow temperature, pH or redox conditions (e.g. prehnite, analcime, alunite, jarosite). The recently discovered alteration mineral diversity suggests global Mars trends were modulated by specific local conditions. Moreover, distinctive stratigraphies and morphologies of the mineral-bearing units suggest multiple settings for liquid water. Here are a few of the earliest

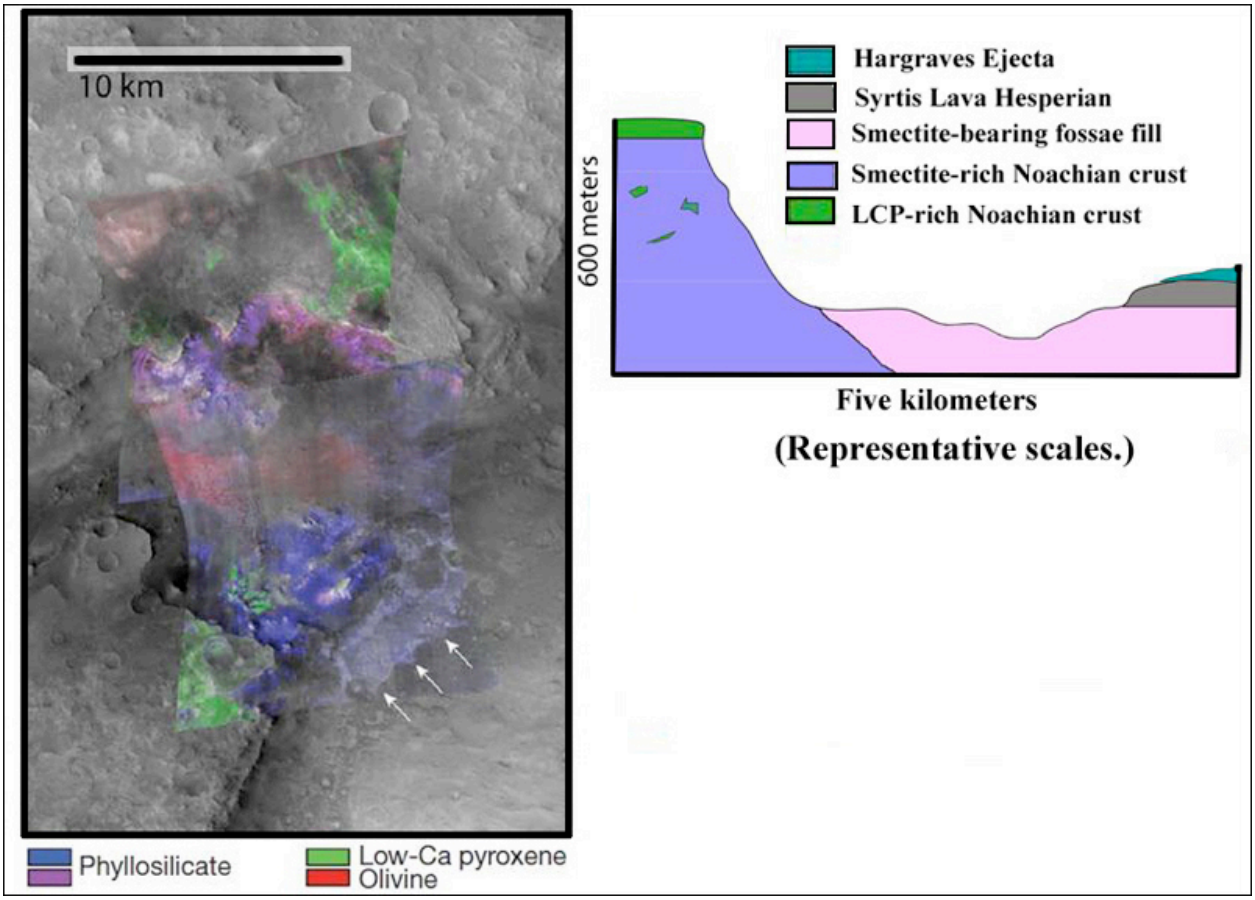


**FIGURE 5.** 'Deep phyllosilicates' as exposed in a 600m tall scarp beneath a mafic LCP-bearing cap rock (figures after Mustard et al., 2008; 2009). Arrows indicate that Fe/Mg smectites exposed beneath the younger Syrtis Major lavas. Olivine is present here in as mobile sands. The two CRISM images are overlain on and use to colorize a grayscale, high resolution Context Imager (CTX) image. Uncolored parts of the image do not have CRISM coverage.

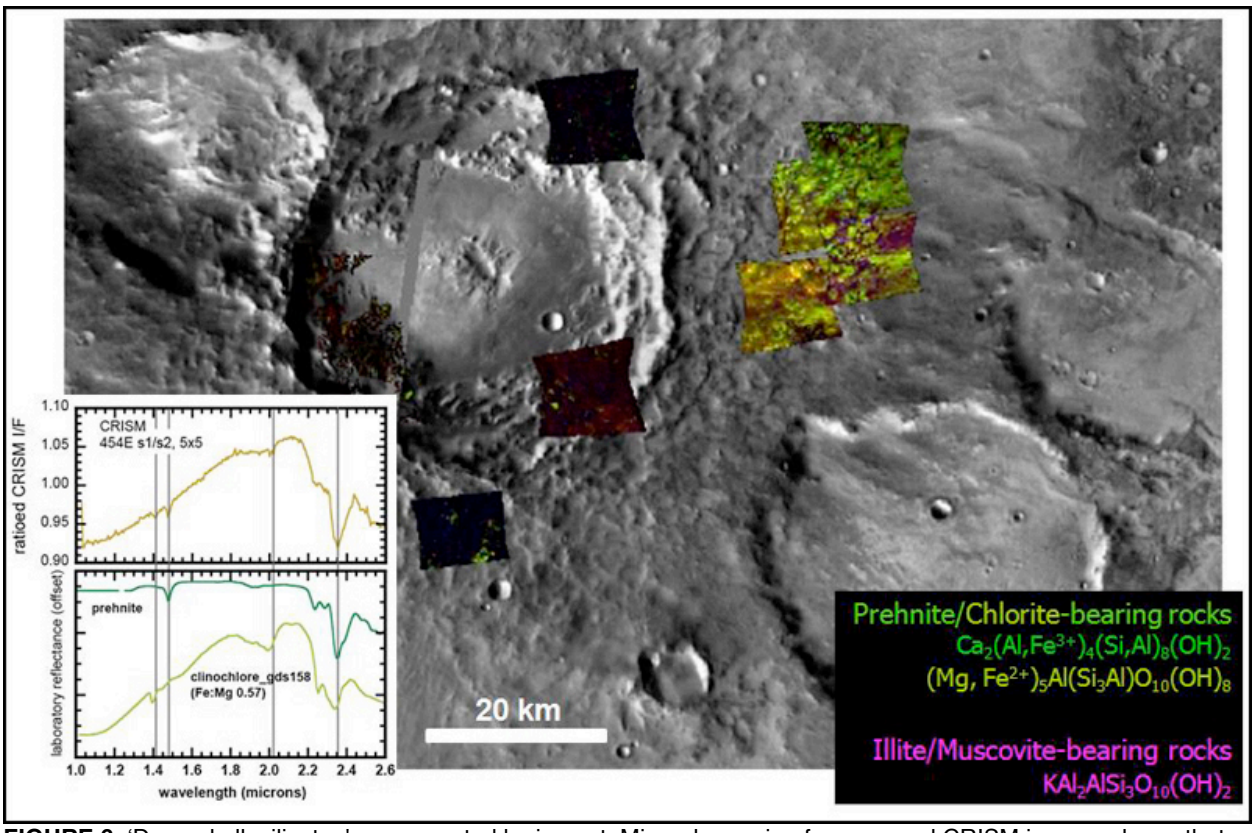


**FIGURE 6.** 'Deep phyllosilicates' as excavated by impact. Mineral mapping from several CRISM images shows that prehnite and chlorite are the spectrally dominant phases in ejecta surrounding this 50km diameter crater (figure from Ehlmann et al., 2009). Where CRISM images are black, no alteration mineral phases were observed during examination of spectra.

environments:

"Deep phyllosilicates": these geologic materials are the oldest altered crust on Mars and, in some areas, such as in the Nili Fossae fracture system, the basement layer of a complex stratigraphy (Figure 5). Here the basaltic materials have been partially altered to materials whose VNIR spectral signature is dominated by that of Fe/Mg smectite clays. The materials are frequently brecciated and sometimes have raised veins and fractures. In this region, these clay-bearing materials are the deepest exposed unit and apparently unaltered mafic materials cap them (Mustard et al., 2009). Elsewhere, hydrated minerals buried deeply in Mars' crust are exposed by craters drilling into the southern highlands and throwing out material. Some of the "deep phyllosilicates" have a distinctively hydrothermal character. Minerals and mineral assemblages indicative of low-grade metamorphism such as analcime, illite, and prehnite are found associated with craters. Figure 6, for example, shows a crater with prehnite- and chlorite-bearing ejecta deposits. Prehnite is a mineral diagnostic of the temperature and pressure of its formation since it only forms at temperatures between about 200-350°C and pressures <3 kbar. That it is in ejecta deposits means that it was most likely transported ballistically during impact, excavating materials from depth, rather than formed in-situ (Ehlmann et al., 2009). "Deep phyllosilicates" may represent the altered component of Mars earliest crust, which was churned by repeated impacts that were a common feature of the early solar system. That the bulk rock and breccia blocks within are altered to smectite clays suggests liquid water was probably stable that time and, at least in some locations, hydrothermal processes were occurring.

"Layered phyllosilicates": Near the two most areally extensive phyllosilicate deposits on

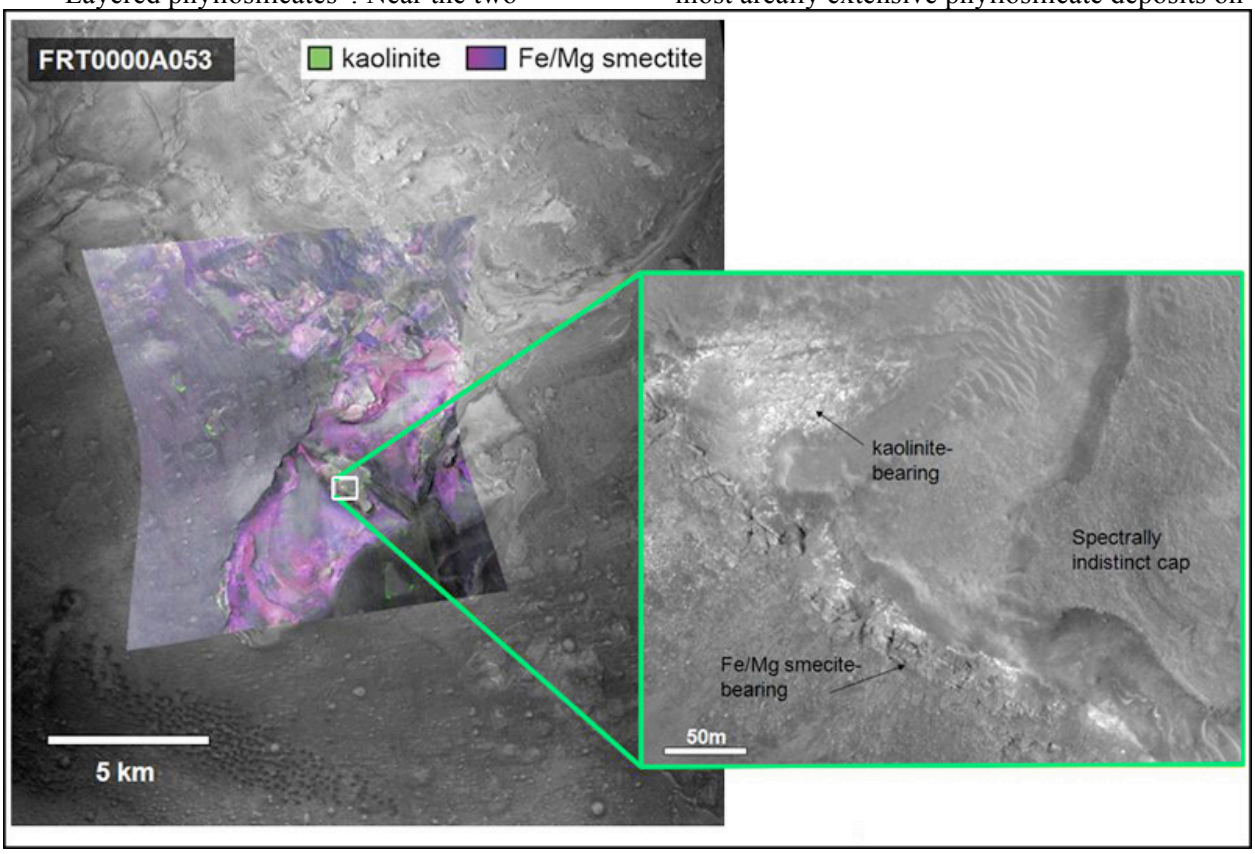


**FIGURE 7.** Example of the layered phyllosilicates. A CRISM parameter map was used to colorize a higher resolution Context Imager (CTX) observation. The 2.3 micron Fe- or Mg-OH absorption in Fe/Mg smectites is mapped as red, the $H_2O$ 1.0 micron band is mapped as blue, and the 2.2 micron Al-OH band is mapped as green. In this filled crater from Nili Fossae, a thin Al-OH bearing unit, identified using spectral data as kaolinite, overlies an Fe/Mg smectitie-bearing unit (figure from Ehlmann et al., 2009).

Mars, at Mawrth Vallis and the Nili Fossae, a distinctive stratigraphy is observed, traceable over hundreds to thousands of kilometers. Alumnium phyllosilicates are found overlying Fe/Mg smectites. Figure 7 shows one example from eroded sediments which fill a crater. The bulk of the sediments are Fe/Mg smectite bearing, but a distinctive bright layer tens of meters thick instead has a spectral signature consistent with a kaolin group mineral most likely kaolinite or halloysite. Elsewhere on Mars, in this Al phyllosilicate layer, kaolinite is accompanied by montmorillonite and opaline silica (Bishop et al., 2008). A simple explanation to explain this stratigraphy is top-down leaching by surface and near surface waters that strips a pre-existing smectite unit of Fe, Mg, and Ca cations, leaving behind mostly Al and Si to form kaolinite (Ehlmann et al., 2009). An analog terrestrial setting is pedogenesis of Hawaiian basalts under intermittently wet conditions.

Carbonate and altered ultramafics: in one region of the planet, near the Nili Fossae an areally extensive stratigraphic unit elevated in olivine abundance (>30%) is found circumferential to the Isidis impact basin (Figure 8). The unit is thought to represent either lavas emplaced immediately following basin formation or a melt sheet containing materials excavated from Mars' lower crust and upper mantle by the impact (Mustard et al., 2009). The olivine-bearing bedrock exhibits signs of partial alteration, in most cases to magnesium carbonate and in a few cases to serpentine (Ehlmann et al., 2009). On Mars, these deposits are significant because the existence of carbonate at this site indicates neutral to alkaline aqueous conditions, in contrast to acid conditions indicated at

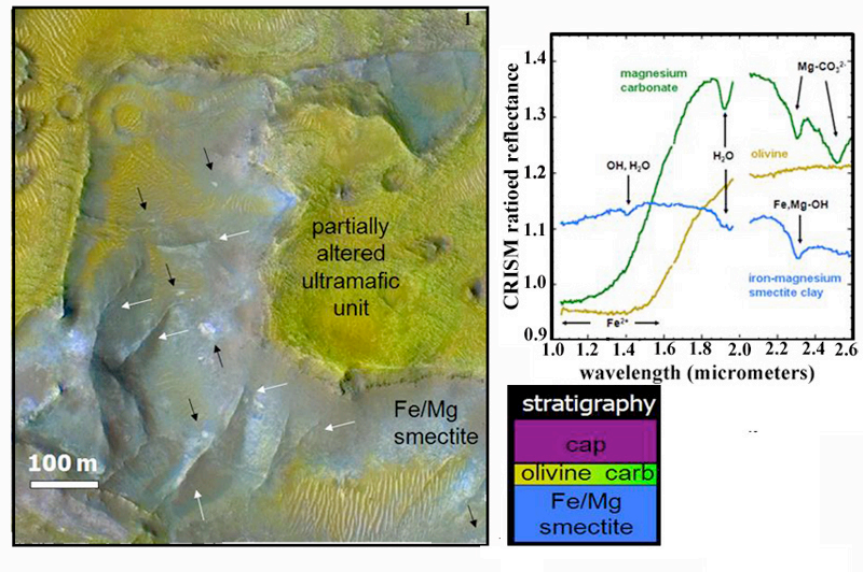


**FIGURE 8.** Example of the partially altered ultramafic unit and phyllosilicate/carbonate stratigraphy. CRISM spectra at the upper right correspond to colored units in this CRISM false color plus grayscale HiRISE (23cm/pixel) composite image. Arrows point to raised fractures (white) and breccia blocks (black) in the Fe/Mg smectite-bearing unit (figure from Ehlmann et al., 2009).

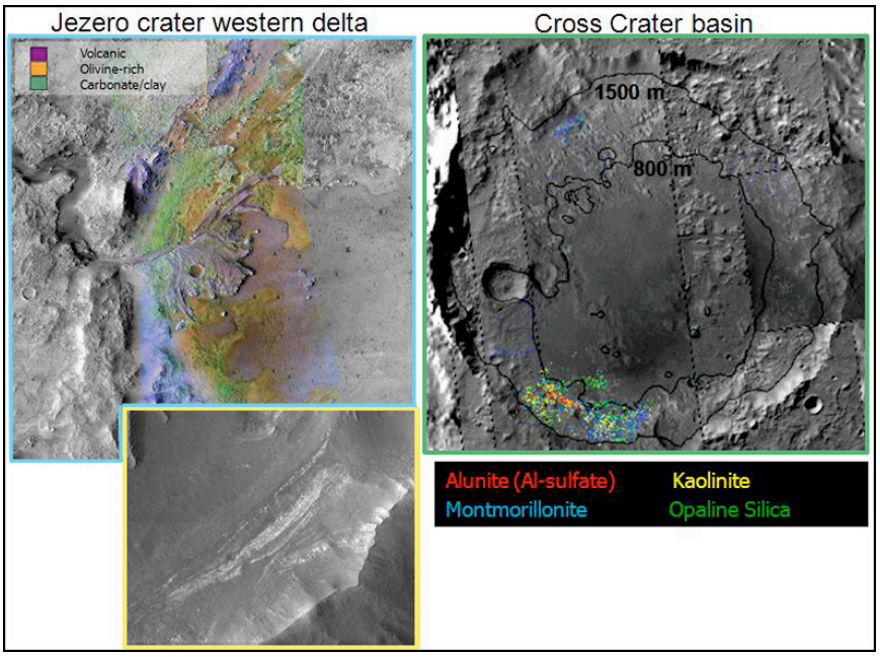


**FIGURE 9.** (left) the western delate of Jezero crater. Sediments within are Fe/Mg smectite and Mg carbonate bearing. The inset shows the wall of the crater in the delta which exposes a 20m crossbedding structure (Ehlmann et al., 2008a). (right) the Cross crater basin hosts layered sediments and where eroded exhibit signatures of alunite, silica, and Al-phyllosilicates (Swayze et al., 2008).

different locations and in younger rocks by the MER rovers (Ehlmann et al., 2008b). Serpentine is also a tantalizing find because the process of serpentinization leads to the generation of methane. Although these particular rocks formed billions of years ago and do not indicate the source for the methane presently observed in the Mars atmosphere, it points to the fact that processes of methane production from serpentinization did exist in Mars' past.

Fluvial/lacustrine sedimentary clays: Craters are topographic lows. A few have hosted crater lakes and still fewer host sedimentary structures that contain alteration minerals. Depending on the basin, however, the preserved sediments differ in mineralogy and implied geochemical conditions. One example is Jezero crater (Figure 9), a putative open basin lake which apparently hosted neutral to alkaline waters. The materials comprising sediments within the crater are

Fe/Mg smectite- and Mg carbonate- bearing similar to the materials found in the Jezero basin watershed (Ehlmann et al., 2008a). Elsewhere, the lakes have a distinctly different acidic character. For example, a closed basin in Terra Sirenum, Cross Crater, probably once hosted a crater lake and is filled with sediments containing alunite, an Al-sulfate that forms only at pH <4 (Swayze et al., 2008). Alunite, along with silica and aluminum phyllosilicates, is found within friable layered units ringing the crater (Figure 9).

The sulfate-forming epoch and its many environments: Salts, e.g. sulfates, become increasingly common and clays less common in later time periods. As revealed by in-situ exploration by the Mars exploration rover at Meridiani Planum, the Hesperian sandstones there have been altered by acidic waters in a complex sequence of surface weathering and diagenesis (Squyres et al., 2004). At Gusev crater, the Spirit rover has found evidence for silica and sulfates possibly created by acid hydrothermal systems (Squyres et al., 2008). Furthermore, extensive silica deposits accompanied by sulfates have been found from orbit in the plains surrounding Valles Marineris and massive mounds of sulfate-bearing materials exist within the Valles system (Milliken et all, 2008; Murchie et al., 2009).

## THE FUTURE

All these discoveries point to the fact that Mars has a rich record from its first billion years available for exploration. On Mars, the new news for scientists is to think locally rather than globally. The types of chemical environments that hosted liquid water varied substantially in character through space and time.

The most immediate impact that these new mineral finds will have on NASA and ESA's program of Mars exploration is in the selection of the landing site for the next rover, the Mars Science Laboratory (MSL) that launches in 2011. Environments of paleolakes with sediments with Fe/Mg smectite clays (Holden and Eberswalde, Gale) and layered phyllosilicates (Mawrth Vallis) are currently represented in the suite of four finalists. In light of recent discoveries of the diversity of alteration environments on early Mars, two additional sites , altered ultramafics (Northeast Syrtis) and a plain of sediments of Fe/Mg smectites and chloride (East Margaritifer), were recently targeted for a period of intensive study for their consideration as candidates [for more on this selection process see http://marsoweb.nas.nasa.gov]. Landing site safety is the primary factor that must be fulfilled at the chosen site and efforts are ongoing to characterize any possible hazards. In addition to finding out more about aqueous processes on early Mars, scientists hope that in-situ sample analysis could reveal evidence for organic carbon (Mahaffy, 2009). Scientifically, an intense debate rages over (a) what types of environments early microbial organisms might have been most likely to inhabit and (b) in which types of environments biosignatures of past life-organic carbon, morphologic fossils, mineral disequilibria, or distinctive isotopic fractions-are most likely to be preserved over three billion years.

In spite of all the progress made since 2004, many questions persist about the newly discovered alteration minerals. One basic question is "how much?" Quantification of mineral abundance with VNIR data is a highly nonlinear problem, since texture and grain size also effect spectra, although efforts are beginning to model likely modal mineralogies (Poulet et al., 2008). Mineralogic data have also thrown down the gauntlet for geochemical modelers to use data on the minerals and their assemblages to more tightly constrain geochemical conditions and the rates and processes of mineral formation so as to establish more detailed parameters on Mars' earliest environments.

As VNIR images from OMEGA and CRISM continue to be collected and analyzed, discoveries of still more minerals on Mars may yet be made. By combining orbital data with data from the next generation of landers and rovers, we can make substantial progress in understanding the history of water on Mars, its evolution over billions of years, and perhaps, whether Mars ever hosted the geochemical environments necessary to sustain life.

## REFERENCES

Bibring, J.-P., et al. (2005), Surface diversity as revealed by the OMEGA/Mars Express observations, Science, 307, 1576- 1581.

Bibring J.-P., et al. (2006), Global mineralogical and aqueous Mars history derived from OMEGA/Mars Express data, Science, 312, 400-404.

Bibring, J.-P., et al. (2007), Coupled ferric oxides and sulfates on the Martian surface, Science, 317, 1206 - 1210.

Bishop, J. L., et al. (2008), Phyllosilicate diversity and past aqueous activity revealed at Mawrth Vallis, Mars, Science, 321, 830 - 833.

Burns, R.G. (1993) Mineralogic applications of Crystal Field Theory Cambridge Univ. Press, 527p.

Christensen, P.R. et al. (2000), Detection of crystalline hematite mineralization on Mars by the Thermal Emission Spectrometer : Evidence for near-surface water, J. Geophys. Res., 105, 9,623-9,642.

Clark, R. N., et al. (1990), High spectral resolution reflectance spectroscopy of minerals, J. Geophys. Res., 95, 12,653-12,680.

Clark, R. N., et al. (2003), Imaging spectroscopy: Earth and planetary remote sensing with the USGS Tetracorder and expert systems, J. Geophys. Res., 108(E12), 5131, doi:10.1029/2002JE001847.

Clark, R. N., et al. (2007), USGS Digital Spectral Library splib06a, U.S. Geol. Surv. Data, 231.

Clark, R. N., et al. (2008), Diversity of mineralogy and occurrences of phyllosilicates on Mars, Eos Trans. AGU, 89(53), Fall Meet. Suppl., Abstract P43D-04.

Ehlmann, B. L., et al. (2008a), Clay minerals in delta deposits and organic preservation potential on Mars, Nat. Geosci., 1, 355- 358.

Ehlmann, B. L., et al. (2008b), Orbital identification of carbonate-bearing rocks on Mars, Science, 322, 1828-1832.

Ehlmann, B. L., et al. (2009), Identification of hydrated silicate minerals on Mars using MRO-CRISM: Geologic context near Nili Fossae and implications for aqueous alteration, J. Geophys. Res., 114, E00D08, doi:10.1029/2009JE003339.

Farrand W.H. et al. (2009) Discovery of jarosite within the Mawrth Vallis region of Mars. Icarus, 204, 478-488.

Gendrin A., et al. (2005), Sulfates in Martian layered terrains: The OMEGA/Mars Express View, Science, 307, 1587- 1591

Hartmann, W. K., G. Neukum (2001), Cratering chronology and the evolution of Mars, Space Sci. Rev., 96, 165-194.

Langevin, Y., et al. (2005), Sulfates in the north polar region of Mars detected by OMEGA/Mars Express, Science, 307, 1584-1587.

Mahaffy, P. (2009) Sample Analysis at Mars <http://www.geochemsoc.org/≥; : Developing Analytical Tools to Search for a Habitable Environment on the Red Planet", Geochemical News, 141.

Murchie, S. L., et al. (2007), Compact Reconnaissance Imaging Spectrometer for Mars (CRISM) on Mars Reconnaissance Orbiter (MRO), J. Geophys. Res., 112, E05S03, doi:10.1029/2006JE002682.

Murchie, S. L., et al. (2009), A synthesis of Martian aqueous mineralogy after one Mars year of observations from the Mars Reconnaissance Orbiter, J. Geophys. Res., 114, E00D06, doi:10.1029/2009JE003342.

Milliken, R.E. et al. (2008), Opaline silica in young deposits on Mars, Geology, 36, 847-850

Mustard, J. F., et al. (2008), Hydrated silicate minerals on Mars observed by the CRISM instrument on MRO, Nature, 454, 305- 309.

Mustard, J. F., et al. (2009), Composition, Morphology, and Stratigraphy of Noachian Crust around the Isidis basin, J. Geophys. Res., 114, doi:10.1029/2009JE003349.

Pelkey, S. M., et al. (2007), CRISM multispectral summary products: Parameterizing mineral diversity on Mars from reflectance, J. Geophys. Res., 112, E08S14, doi:10.1029/2006JE002831.

Poulet, F., et al. (2005), Phyllosilicates on Mars and implications for early Martian climate, Nature, 438, 623-627.

Poulet, F., et al. (2008), Abundance of minerals in the phyllosilicate-rich units on Mars, Astron. Astrophys., 487, L41 -L44, doi:10.1051/0004-6361:200810150.

Roach, L. H., et al. (2009), Testing evidence of recent hydration state change in sulfates on Mars, J. Geophys. Res., 114, E00D02, doi:10.1029/2008JE003245.

Squyres, S. W., et al. (2004), In-situ evidence for an ancient aqueous environment at Meridiani Planum, Science, 306, 1709-1714.

Squyres S.W., et al. (2008), Detection of silica-rich deposits on Mars: Science, 320, 1063- 1067.

Swayze G.A. et al. (2008), Eos Trans. AGU, 89(53), Fall Meet. Suppl., Abstract P44A-04

**Introduction by Paul Mahaffy (NASA Goddard Space Flight Center)**

Volumes of multispectral infrared imaging data presently flowing in from Mars orbiting spacecraft are giving us a new view of the planet (Ehlman, Geochemical News 142) and pointing toward candidate landing sites for surface rovers. Highly ruggedized and miniaturized instruments on future rovers will carry out an even more detailed exploration of the chemistry and mineralogy at the most interesting sites to elucidate geological and geochemical processes that may point toward habitable environments for past or present life. One such instrument planned for use on the Curiosity rover that is planned to land on Mars in 2012 is the x-ray fluorescence/x-ray diffraction instrument CheMin described in this contribution from the Principle Investigator for this investigation, David Blake. Some of the robust field-testing of this instrument on remote Mars analog sites in the Arctic Svalbard archipelago is also described.

# A historical perspective of the development of the CheMin mineralogical instrument for the Mars Science Laboratory (MSL '11) Mission

**David BLAKE**[a]
[a]NASA Ames Research Center

## INTRODUCTION

In our solar system, Mercury, Venus, Earth and Mars are rocky planets; Jupiter, Saturn, Uranus and Neptune are gas giants with no solid surfaces, and Pluto (now, sadly, demoted to "planetesimal" status) is icy and cryogenically cold. Early in Solar System history, surface conditions on Mars and Venus diverged from what could have been a "habitable" status. Venus is not presently habitable due to its high surface temperature and inhospitable atmospheric composition. Furthermore, present day surface temperatures and atmospheric conditions on Venus would have likely destroyed any evidence of earlier habitable conditions. Mars cooled off and lost most of its atmosphere, but still preserves geological evidence of its early history - a time when its climate was much more clement than the present day. With the exception of "special" zones such as the proposed subsurface ocean of Jupiter's moon Europa or the organic-rich surface of Saturn's moon Titan, "habitable zones" are more or less confined to the surface and near-surface environments of Earth and Mars. For the foreseeable future then, Mars seems to be the most promising place in the solar system to look for evidence of past or present extraterrestrial life.

An important difference between Mars and Earth is the apparent absence of extensive plate tectonics on Mars. On Earth, as a result of plate tectonic movements, most surface crustal components older than ~3 billion years have been subsumed by convergent plate margins or metamorphosed beyond recognition of origin or both. Truly ancient crust that existed in the habitable zone when early terrestrial life developed and radiated can only be found in highly deformed slivers of rocks in a few places in the world. By contrast, much of the Mars surface from that early epoch has been preserved relatively unaltered. Thus, there is the possibility on Mars to study relatively unaltered crust in which habitable zones were preserved at the time when terrestrial life originated and radiated.

Our recent knowledge of early geology and potentially habitable environments on Mars is derived from decades of study of Mars meteorites such as ALH 84001, from the orbital observations of Mars Observer, Mars Reconnaissance Orbiter and the European Space Agency's Mars Express Orbiter, from Mars Pathfinder and from the Mars Exploration Rovers. We hope to continue the rich heritage of Mars science during the upcoming Mars Science Laboratory Mission.

## THE MARS SCIENCE LABORATORY MISSION

Mars Science Laboratory (MSL '11) is NASA's follow-on landed mission to the Mars Exploration Rovers *Spirit and Opportunity,* which, more than 6 years after their intended 90-day lifetimes, are still making fundamental scientific discoveries on the Mars surface. MSL is intended to "…Explore and quantitatively assess a local region on the Mars surface as a potential habitat for life, past or present." The duration of the primary mission of MSL will be 670 sols, or one Mars year (about two Earth years). During this time, the plan is for the MSL rover (named "Curiosity") to traverse to at least 3 geologically distinct sites within its 20 km diameter landing ellipse and determine the "habitability" of these sites (habitability is defined in this context as the "capacity of the environment, past or present, to sustain life").

The CheMin instrument will be principally engaged in the following MSL science objectives:

- Characterizing the geology and geochemistry of the landed region;
- Investigating the chemical and mineralogical composition of Martian surface and near-surface geological materials;
- Interpreting the processes that have formed and modified rocks and regolith.

MSL carries four types of instruments: "Environmental instruments" such as the Radiation Assessment Detector ("RAD") and the Rover Environmental Monitoring Station ("REMS"), "remote observation" instruments such as the Mast Camera ("Mastcam"), the Mars Descent Imager ("MARDI") the Chemistry-and-Camera ("ChemCam") and the Dynamic Albedo of Neutrons ("DAN"), and "arm instruments" including the Alpha Particle X-ray Spectrometer ("APXS") and the Mars Hand Lens Imager ("MAHLI"). Inside the body of the rover is the "Analytical Laboratory" which is comprised of the Chemistry and Mineralogy ("CheMin") instrument and the Sample Analysis at Mars ("SAM") instrument suite. Each of these instruments, as well as the mission itself, is described in detail on the MSL mission website.[1]

Together, the environmental, remote and arm instruments of *Curiosity* operate much like a field geologist would on Earth – identifying interesting rocks or formations from a distance (even obtaining an elemental analysis from up to 10 meters using ChemCam), then approaching them to make *in situ* hand lens observations and elemental analyses. These operations and observations are similar to those performed by *Spirit* and *Opportunity* for the past 6 years. However, once these operations are performed, *Curiosity* goes further. *Curiosity* can collect, prepare and analyze samples in much the same way that this is done in a terrestrial laboratory. When a sample is found to be interesting by scientists on Earth, *Curiosity* will deploy an arm-mounted percussion drill called "PADS" (Powder Acquisition Drill System) in concert with a sample processing system called "CHIMRA" (Collection and Handling for Interior Martian Rock Analysis) to collect material for further analysis. Drilled or scooped material is then sieved and a portion of this sieved material is transferred to the Analytical Laboratory. *Curiosity's* Analytical Laboratory can conduct quantitative mineralogical analysis (CheMin) and organic and isotopic analysis (SAM) of material delivered through funnels into the body of the rover. Once a complete analysis is obtained by the Analytical Laboratory, results are sent back to Earth for interpretation.

## HOW DOES CHEMIN WORK?

CheMin determines the mineralogy of crushed or powdered samples through X-ray diffraction (XRD) and elemental composition through X-ray Fluorescence (XRF). XRD is an extraordinarily powerful technique that identifies the structures of crystalline materials from first principles, and is the preferred method for mineralogical analysis in terrestrial laboratories.

During a mineralogical analysis, a ~50 µm collimated X-ray beam from an X-ray tube source is directed through powdered or crushed sample material. An X-ray sensitive CCD imager on the opposite side of the sample from

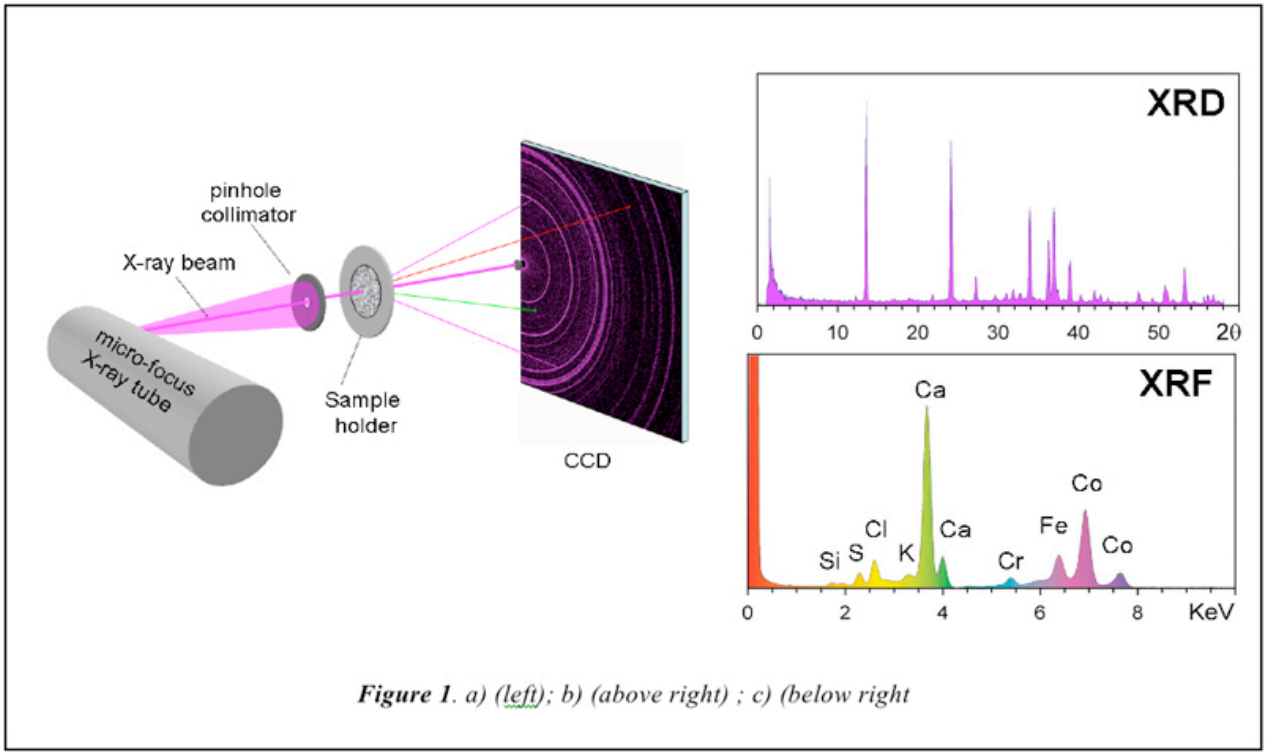


***Figure 1**. a) (left); b) (above right) ; c) (below right*

**Figure 1.** Geometry of the CheMin XRD/XRF instrument. a) (left) overall geometry of CheMin; b) (above right) XRD 2q plot obtained by summing diffracted photons from the characteristic line of the X-ray source (colored magenta in Figure 1a); c) (below right) X-ray fluorescence spectrum obtained by summing all of the X-ray photons detected by the CCD (XRF photons from the sample shown schematically in green and red in Figure 1a).

the source directly detects X-rays diffracted or fluoresced by the sample (Figure 1a) [Details of the CCD operation are shown in Appendix A].

During an X-ray Diffraction analysis, CheMin's CCD detector is exposed to the X-ray flux, read out and erased many times (100-1000 exposures). The detected X-rays are used to produce both diffraction and fluorescence data. Diffracted primary beam X-rays strike the detector and are identified by their energy. A two-dimensional image of these X-rays constitutes the diffraction pattern (Fig. 1a). At incremental radii this pattern is summed circumferentially about the central undiffracted beam to yield a 1- dimensional 2q plot comparable to conventional diffractometer data (Fig. 1b). All of the X-rays detected by the CCD are summed into a histogram of number of photons vs. photon energy that constitutes an XRF analysis of the sample (Fig. 1c).

The requirement for CheMin to perform X-ray Fluorescence (XRF) elemental analysis was removed early in the spacecraft instrument design phase. The energy-dispersive X-ray histograms obtained during an analysis will only be used to construct energy-selected diffraction patterns, such as CoKa. When this is done, sample fluorescence, multiple photon detections in a single pixel, tracks from cosmic rays, etc. can be removed from the patterns. While the requirement to perform XRF elemental analyses was descoped by the MSL project, these data are still obtained by the instrument and will be analyzed on a "best effort" basis.

Quantitative mineralogical results are obtained from XRD data by Rietveld refinement and other full-pattern fitting techniques.[2,3] Both crystalline and amorphous materials can be analyzed in this way. The duration of a single XRD experiment sufficient to quantitatively analyze a single mineral such as quartz or olivine, is less than one hour and consumes a few tens of Watts. Complex assemblages such as basalts having 4 or more minerals plus glass may require the summation of 4–8 of these experiments over 1 or more Mars sols.

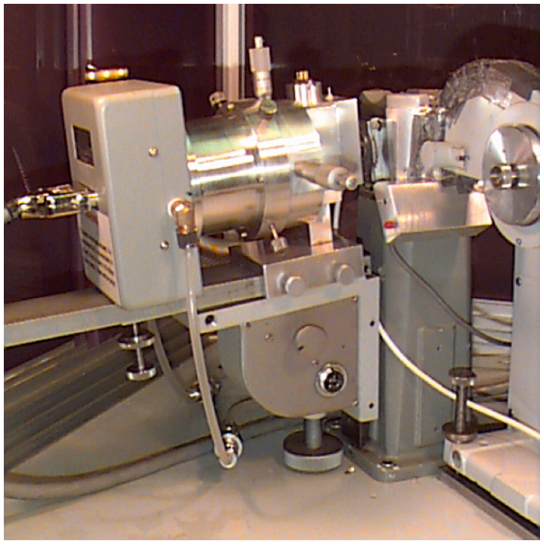

**Figure 2 (a).** CheMin I instrument. A Princeton Instruments™ camera is interfaced to an evacuated sample chamber. A modified collimator from a Debye-Scherrer powder camera provided a 50 $\mu$m diameter collimated beam. X-rays are provided by a Norelco-Philips Tube tower. The detector is a Tektronix TK-512 backthinned, back illuminated 512 X 512 pixel CCD imager. Initially, analyses required several thousand CCD frames, with a total energy of thousands of watts hours. Since the sample chamber had to be taken apart to load samples, it typically took several days to align the X-ray beam after sample exchange. Power supplies, X-ray generator, camera controller and chilled water supplies for the X-ray tube tower and camera are not shown.

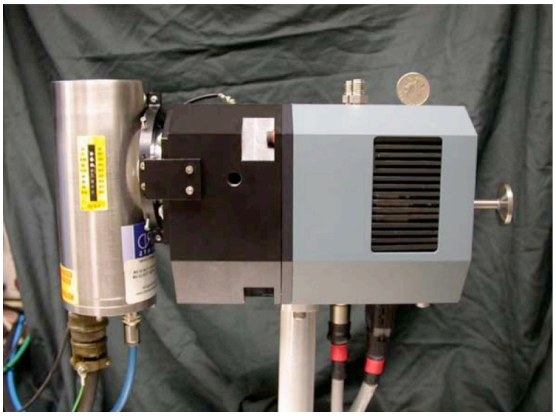

**Figure 2 (b).** CheMin II instrument. The instrument consisted of an Andor™ CCD camera interfaced to a sample chamber (kept at atmospheric pressure), bolted to an Oxford X-ray Technology Group micro-focus X-ray tube. The detector is an E2V 5530 1250 X 1150 pixel CCD imager. Samples could be exchanged in air, without disturbing the alignment of the instrument. Power supplies for the X-ray tube and camera are not shown. The instrument is air cooled.

## PROTOTYPES AND TERRESTRIAL ANALOGS OF THE CHEMIN INSTRUMENT

During the development of the CheMin instrument concept, several prototypes were built which had increasing fidelity to what would become the flight instrument. The CheMin I instrument consisted of a commercial CCD camera in an evacuated housing with rudimentary sample handling mechanisms, interfaced to a commercial X-ray tube tower (Fig. 2a). An evacuated housing was necessary because the CCD was cooled to -60° C during operation. he electronics and power supplies for this machine – and the X-ray source – occupied a small room. CheMin II was an improvement relative to CheMin I in that a self-contained X-ray tube and power supply was interfaced to a sealed and evacuated commercial CCD camera (Fig. 2b). A thin beryllium window allowed X-rays to enter the camera and expose the CCD. Because the samples were analyzed in room air, we could experiment more freely with sample types and sample delivery / sample movement mechanisms.

A breakthrough in sample handling occurred between CheMin II and III. For a sample to be optimally prepared for powder XRD, it must be ground to somewhat less than 10 µm particle size, a difficult task even in terrestrial laboratories (this is basically the same grain size as flour or face powder). The reason for this is that in order to get a pattern with all diffraction peaks present at their correct intensities, random orientations of myriads of tiny crystallites are required. We had experimented with finely ground pressed powders translated with an x,y stage, but nothing seemed to work particularly well. CheMin Co-I Philippe Sarrazin proposed a sample holder in which loose powder is held between two X-ray transparent plastic windows spaced ~200 µms apart. By vibrating the sample holder at sonic frequencies with a piezoelectric device, (we first used modified buzzers from Radio Shack) the powder was made to flow like a liquid inside the cell. This solved our two most difficult sample handling problems – exposing a representative amount of the sample to the 50

µm diameter X-ray beam during the analysis, and rotating the grains to all orientations as they passed through the beam. We found that powders ground and sieved to less than 150 µm diameter produced excellent patterns. Rock powder produced by a variety of techniques (drilling, grinding, crushing) has a significant fraction in this size range and below.

CheMin III was our first field demonstration model, and consisted of the basic components of CheMin (X-ray tube, Sample handling system and CCD camera) held in a portable frame along with control electronics and power supplies (Fig. 2c). The instrument was powered through a cable connected to several motorcycle batteries, and operated through a laptop computer. CheMin III was demonstrated in Death Valley, CA in 2003. However, the entire system still occupied the trunk of a car and had limited durability at remote localities. CheMin IV was the first truly portable CheMin system. While it appears much like the earlier model, it was operated by an integrated microcomputer and powered by on-board Li-ion batteries and a power management system. Data were transferred to a laptop computer using a USB thumb drive, and processed off-line. CheMin IV was used to obtain the first remote quantitative mineralogical analysis by David Bish of Indiana University during a field expedition to Svalbard, Norway, in 2006 (Fig. 2d).

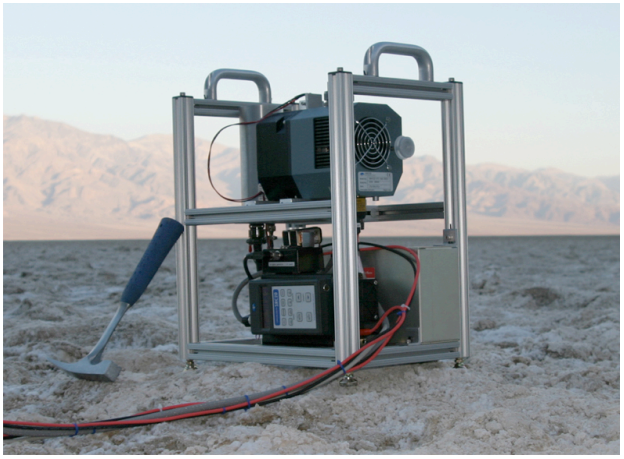

**Figure 2 (c).** CheMin III. The instrument is shown in operation in Badwater Basin, Death Valley in 2003. The X-ray tube and camera are the same as used in CheMin II, however, miniature power supplies and camera control electronics are housed in a portable frame with the instrument. Samples are moved by piezo-shaking in a mylar film-bounded transmission cell. Not shown are storage batteries and laptop computer that provide power and instrument control. Data are collected as individual frames and analyzed off-line by the laptop computer.

**Figure 2 (d).** CheMin IV. (left) As deployed in Svalbard, Norway in 2006. (right) CheMin Co-I Dave Bish of Indiana University performs the first complete XRD/XRF data collection and quantitative analysis in the field. The instrument is fully self-contained, operated with an integrated computer and on-board lithium batteries and power supplies. Once an analysis is completed, the raw data are downloaded onto a USB storage drive and transferred to a laptop computer for processing.

## THE CHEMIN FLIGHT INSTRUMENT

Building a successful flight instrument is a task that is breathtakingly hard, and best left to professionals. MSL instruments are required to operate for a full Martian year on the Mars surface, in temperatures that vary from -70 C to +50 C (instruments outside the body of the rover are required to survive temperatures as low as -130 C). They must survive intense vibration during launch, transit to Mars in vacuum and ultimately operate under varying thermal and atmospheric conditions, as well as survive the intense neutron flux from the DAN instrument and from *Curiosity's* Radioisotope Thermoelectric Generator (RTG). Every fastener and component is tested under the full range of conditions and spares of critical components are "life-tested" for 1.5 times the nominal mission duration. The CheMin flight instrument (also called the "Flight Model," or "FM") was built by scientists, engineers and technicians at NASA's Jet Propulsion Laboratory during 2005-2009, and delivered to the MSL project in June, 2010. A CheMin

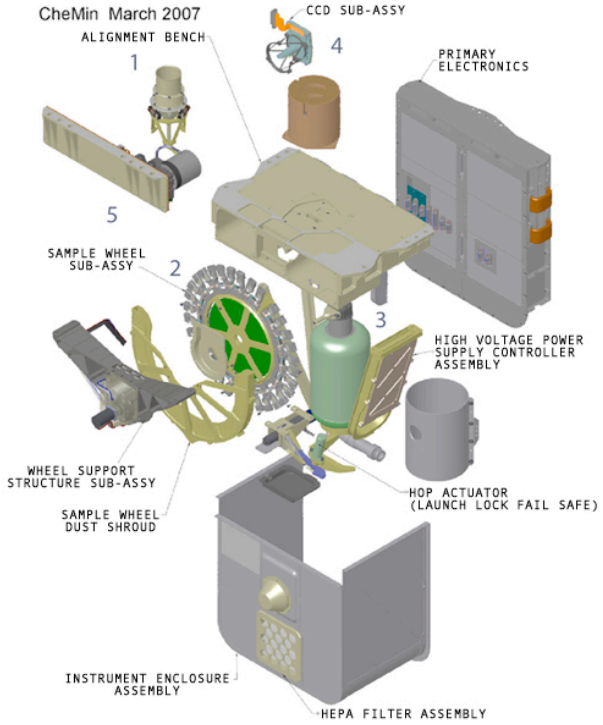


**Figure 3.** Exploded view of CheMin spacecraft instrument. Major components of the instrument are labeled: (1), sample delivery funnel; (2), sample wheel containing 32 sample cells; (3), X-ray tube and collimator housed in pressurized $SF_6$ dielectric (tube, collimator and 28 KV high voltage power supply weigh less than 1 Kg); (4), CCD imager with support structure; (5), CCD housing with cryocooler. Other components include electronics, sample wheel drive motor, etc. The entire instrument, which is essentially a 10" cube, weighs ~10 Kg and operates on ~40 watts.

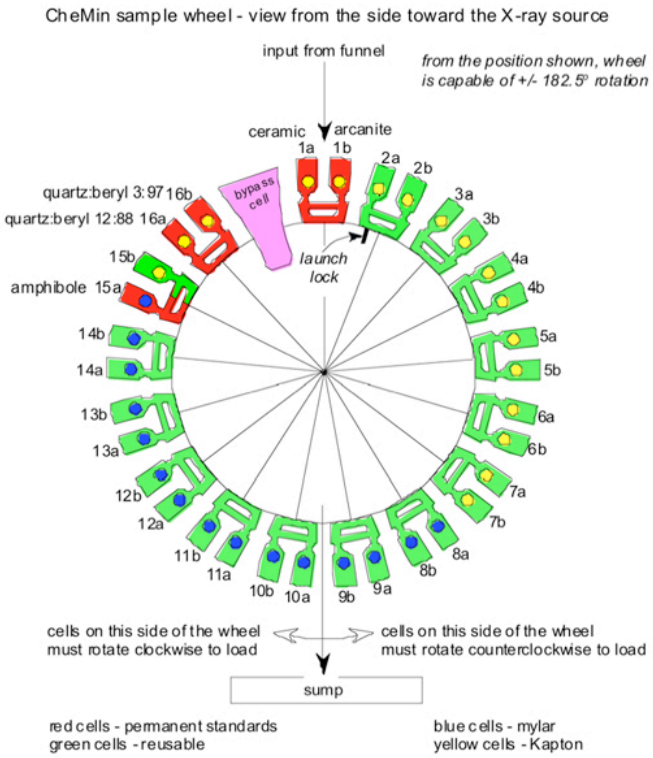


**Figure 4.** Sample wheel. Sample cells (27 total) are loaded and analyzed at the top, then rotated 180 degrees and dumped in the sump after analysis. Permanent reference standards (5 total) are shown colored red, green cells are available for analysis of unknowns. The "bypass cell," shown in pink, is used to pass multiple sample aliquots through the funnel for contamination reduction by dilution. Similarly, individual sample cells can be loaded, shaken and dumped without analysis, then refilled to dilute any contamination that may be present in the cell from previous analyses. If necessary, cells can be used 3 or more times during the

"Demonstration Model", or "DM" is also being constructed that is an exact copy of the FM, and will be used for testing Mars analog samples, as well as for studying potential instrument anomalies during the MSL mission.

An exploded view of the spacecraft instrument is shown in Fig 3. The CheMin sample handling system consists of a funnel, a sample wheel (which carries 27 reusable sample cells and 5 permanent reference standards), and a sample sump where material is dumped after analysis (Fig. 4). CheMin receives sieved drill powders or scoop samples from PADS/CHIMRA [Details of sample delivery and processing are described in Appendix B].

A full analysis of an individual sample is called a "major frame" and will require as many as 10 hours of analysis time, accumulated over multiple sols. Once a major frame of data is sent to ground and accepted, the analyzed material is emptied from the cell and that cell is ready to be reused. CheMin does not have the capability to store previously analyzed samples for later re-analysis [Details of CheMin sample handling and analysis are described in Appendix C].

## X-RAY DIFFRACTION MODE

The CCD is placed in the forward-scattered direction relative to the X-ray beam so that mineral phases with large interplanar spacings (and hence narrow diffraction cones at low 2q), such as clays, can be detected. In addition, low-index lines (which are commonly the most intense and most definitive for phase identification) occur in the forward-scattered direction. Table 1 shows the expected 2q range (for Co Ka radiation) and 2q Full Width at Half-Maximum (FWHM ) for X-ray diffraction.

A special case of X-ray detection by the CCD is the detection of Co Ka characteristic photons from the primary source. When Co Ka photons are detected, the X,Y pixel location on the CCD is identified and the corresponding X,Y location in a 600x582 counting number array is incremented by one. This process results in a Co Ka diffraction image. Various strategies are used in on-board data processing to optimize the quality or quantity of diffraction data returned (e.g., "single pixel" detection, and "split pixel" detection, etc.

An additional 600x582 array stores an image of all of the photons detected by the CCD regardless of energy. This array acts very much like a piece of photographic film, recording the Co Ka XRD pattern as well as background, X-ray Fluorescence from the sample, and Bremsstrahlung radiation from the X-ray source.

## XRD/XRF CALIBRATION AND CHARACTERIZATION

Five permanent cells are loaded with calibration standards (Fig. 4). Three of these cells are loaded with single minerals or a synthetic ceramic and two are loaded with differing quartz/beryl mixtures. Basic calibration, completed prior to delivery of the instrument to MSL Assembly, Test, and Launch Operations (ATLO), was performed using only the five permanent standards loaded into the sample cells of the FM.

Calibration of these standards entails measurement of 2q range and 2q FWHM for XRD, and of the required XRF energy range and

**Table 1.** Diffraction pattern range and peak resolution (for CoKa radiation) of the CheMin FM. Range and resolution were chosen to allow for the successful identification and quantification of virtually all minerals.

| Parameter | Source and Detector Characteristics |
|---|---|
| 2θ range | 5-50° 2θ (Co radiation) |
| 2θ resolution | <0.35° 2θ (measured value = 0.30° 2θ) |
| Operating Voltage | 28 KeV |
| Total Flux | > ~ 5.63 e5 photons/ sec |
| CCD Energy Range | 1-15 KeV |
| CCD Energy Resolution @ 6.93 KeV | < 250 eV |

**Table 2.** CheMin FM mineralogical analysis requirements. Analytical capabilities are defined by a "flow down" of requirements derived from the science goals and objectives of the mission.

| Parameter | Value |
|---|---|
| Mineral Detection Limit | <3 wt. % |
| Mineral Quantification (Accuracy) | <15% of amount present @ 4X detection limit |
| Mineral Quantification (Precision) | <10% of amount present @ 4X detection limit |

FWHM for elemental peaks, in particular Fe Ka, Co Ka and Co Kb. Quantitative accuracy, precision and detection limits are evaluated using the quartz-beryl standards (CheMin's requirements for detection limit, accuracy and precision of analyses are shown in Table 2). Figures 6-7 show data from Cryo-Vac tests of the flight instrument. Fig. 6a-c show single frame, minor frame and major frame data from the amphibole standard. Fig. 6d shows an energy dispersive X-ray histogram for a single frame, and Fig. 6e shows the energy dispersive X-ray histogram for all of the single frames summed into the major frame. Figure 6f shows a 1-D diffractogram obtained for a major frame (full analysis) of the amphibole. Figure 7 illustrates the "best case" X-ray Fluorescence capability of the instrument. These data were obtained by analyzing the synthetic ceramic standard, prepared to evaluate the XRF capability of the instrument.

## QUANTITATIVE XRD CALIBRATION OF THE DEVELOPMENT MODEL (DM) AND OTHER CHEMIN TESTBEDS

Quantitative XRD (QXRD) calibration will be performed using the DM and various other testbeds. For QXRD calibration, synthetic mixtures that mimic real samples likely to be encountered on Mars have been prepared from minerals mixed in known weight fractions, or natural materials of known composition.

For characterization of CheMin operation across a broad spectrum of samples, synthetic and natural, the DM will be supported by testbeds and facilities that replicate various parts of the DM/FM function with varying levels of fidelity:

*The Development Model:* The DM will be set up in a testbed configuration at JPL in CheMin Co-I Albert Yen's laboratory. Prior to launch, the DM will be used to test algorithms, establish calibrations, develop operation scenarios, and characterize Mars analog samples. During landed operations the DM unit will be used to test new command sequences, develop operational scenarios, characterize Mars analog samples and reproduce any instrument anomalies that might occur during the MSL mission.

*Analytical facility for Mars analog rocks:* The Planetary Mineralogy and Spectroscopy Laboratory at NASA Ames Research Center (ARC) will house several CheMin analog instruments. The principal instruments in this laboratory are a CheMin IV instrument[4] and a Terra instrument[5] (a field-deployable instrument based on the CheMin design that was developed by InXitu, Inc). These instruments will be used to analyze Mars analog rocks in a geometry similar to the CheMin FM and the DM instruments. A commercial Inel™ X-ray diffractometer at Ames Research Center is configured to analyze Mars analog rocks in a geometry nearly identical to the CheMin flight instrument. This instrument is equipped with a Co X-ray tube and a 120-degree parallel detection system capable of collecting XRD patterns with a higher 2q resolution than the spacecraft instrument (but which can be degraded to MSL CheMin resolution for comparison and pattern matching). A Mars atmospheric pressure chamber is installed with a carousel and MSL funnel, and a CheMin transmission sample cell capable of being filled, piezo-electrically shaken during analysis and dumped. A large number of patterns of Mars analog rocks and soil are being collected for

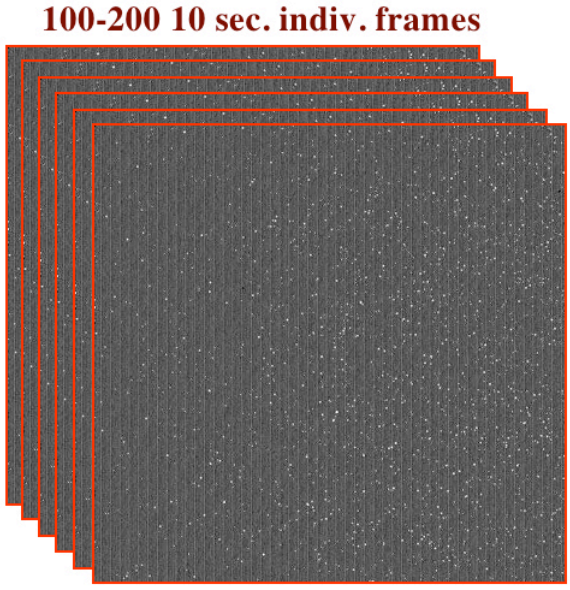


**Figure 6 (a).** Stack of raw single frames (10-second exposures) of 600X582 pixel CCD data. Each frame is background subtracted, and shows individual X-ray photon detections as white or gray spots. In any single exposure, only a few hundred pixels out of 350,000 record X-ray photon detections.

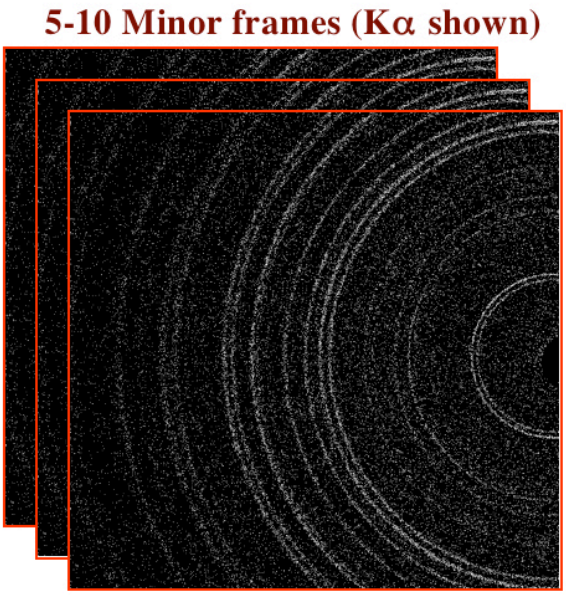


**Figure 6 (b).** Stack of energy-selected CoKa minor frames of CCD data. Each minor frame is a 600X582 array in which the x,y array elements store the integer sum of CoKa photons detected at that x,y pixel location during 100-200 individual frames (exposures).

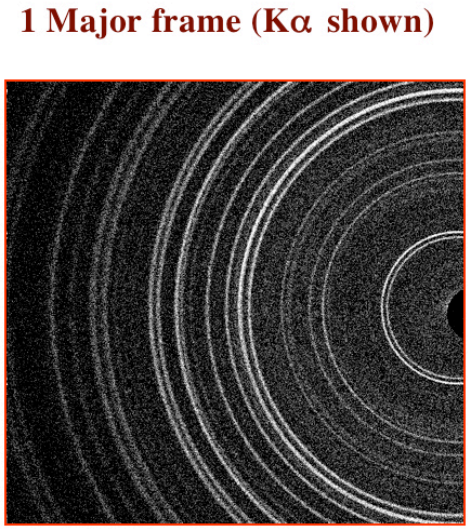


**Figure 6 (c).** Major frame of CCD data, representing the sum of the minor frames. Major frames are used to construct a 2-D diffraction pattern that is translated into a more conventional 1-D diffractogram used for mineral identification and quantitative analysis. Minor frames are used to estimate the precision and accuracy of an analysis and to detect instrumental drift and transient anomalies in the data can be identified and removed.

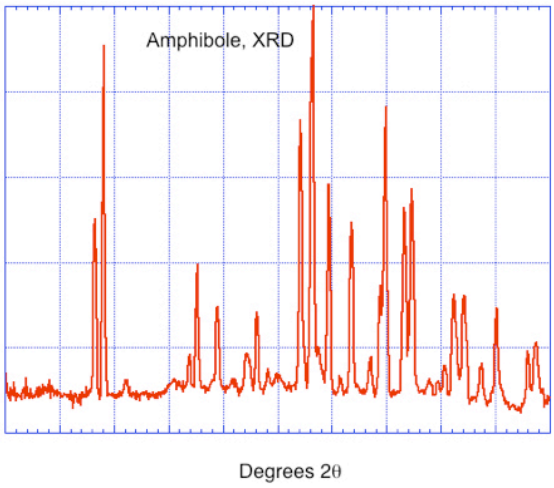


**Figure 6 (d).** 1-D diffractogram constructed from a major frame of CCD data. Intensities from the 2-D pattern are summed circumferentially about the central beam to create an intensity vs. 2q diffractogram, similar to that obtained in conventional powder X-ray diffractometry. The diffractogram shown is from the mineral amphibole, one of the reference standards in the CheMin FM.

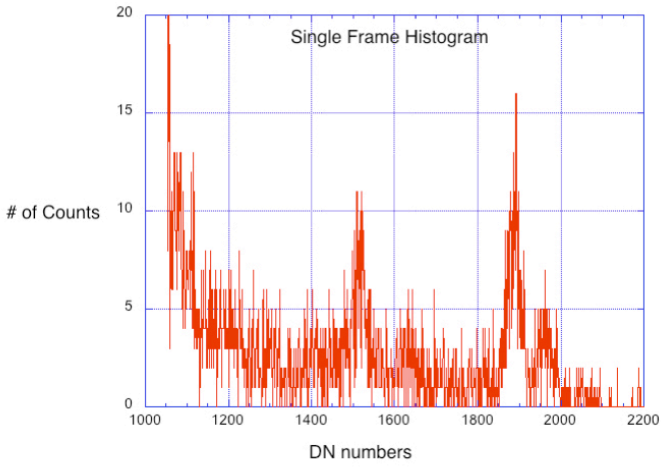


**Single frame histogram**

**Figure 6 (e).** Raw Energy-Dispersive X-ray (EDX) histogram of a single frame of CCD data. The x-axis represents X-ray photon energy and the y-axis represents the number of counts per unit energy (in this case, represented as "DN" or digital numbers from the CCD). Observed peaks include the primary CoKa flux at ~1960 DN, sample-generated FeKa at ~1890 DN, and sample-generated CaKa and CaKb at ~1525 and ~1640 DN respectively.

**Figure 6 (f).** Summed EDX histogram for major frame of CCD data. The X-axis is now converted from DN to energy in thousands of electron volts (KeV). Elemental peaks present include CoKa (6.92KeV), CoKb (7.70 KeV), FeKa (6.4 KeV), TiKa (4.51 KeV), TiKb (4.93 KeV), CaKa (3.68 KeV), CaKb (4.01 KeV), ArKa (2.96 KeV), SiKa (1.75 KeV) and AlKa (1.49 KeV). Fe, Ti and Ca are elements detected from the sample. Argon originates from the 10 mbar of Ar present in the FM during the analysis, Si originates from the detector itself and Al is generated from the light shield in front of the detector. The CheMin instrument is sensitive to elements above ~ Z=15 (phosphorus). While the CCD itself is supremely sensitive to low-energy X-rays such as AlKa, the transmission geometry of the instrument and the presence of a light shield precludes detection of these elements.

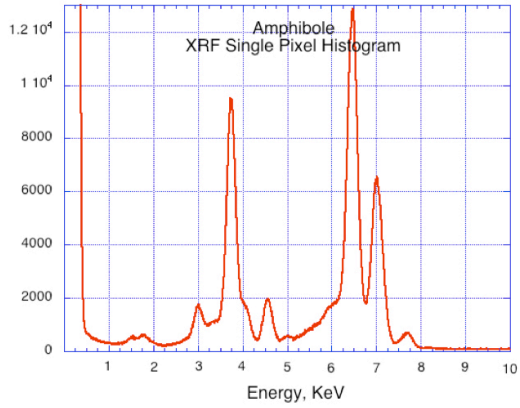


**XRF spectrum**

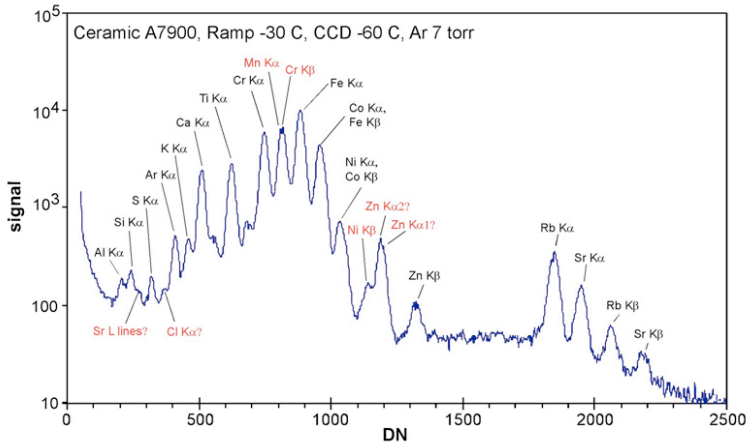


**Figure 7.** A synthetic ceramic was developed as a permanent standard for the instrument. This sample is used to measure the energy response of the CCD detector to sample-generated X-rays. X-ray sensitivity appears to be quite good from Sr to S (Al and Si are instrument generated). The FWHM of individual X-ray peaks, and ultimately X-ray detection and discrimination will be degraded by neutron damage from the RTG during the mission.

analysis prior to, during and after the prime MSL mission. The CheMin IV and Terra instruments have the resolution and diffraction geometry of the MSL Flight instrument and will be used in supporting tests.

## CHEMIN INSTRUMENT MODES

During a nominal 10-hour analysis, CheMin collects and stores X-ray data as individual 600x582 pixel CCD images of 5-30 seconds exposure each. A "minor frame" consists of 30 minutes of these images, nominally 360-60 frames depending on integration time. A complete 10-hour analysis of a sample comprises 20 such minor frames and is called a "major frame."

There is insufficient bandwidth to deliver all of CheMin's raw data to Earth. When commanded, CheMin will deliver raw data to the Rover Compute Element (RCE) that in turn partially processes the raw data for each minor frame, in order to reduce the data volume. Each minor frame of data transmitted to Earth contains one or more raw frames in order to assess the health of the detector, a variety of engineering and health information about the instrument, and one or more of three possible processed data products. The three types of data products are described below:

- "Fully processed mode": Each image is reduced to a pixel map containing ones and zeros, where "1" represents the detection of a photon within a specific energy window (e.g., Co Ka), and "0" represents everything else. Each pixel map is summed into a 600x582 counting number array of pixel positions; the result is a 2-D energy-filtered diffraction pattern. In addition to the energy-filtered diffraction pattern, "fully processed mode" also provides a histogram of all of the photons detected vs. energy, which amounts to an X-ray energy-dispersive spectrum of the sample material.
- "Film mode": Each image is summed into a 600x582 array as raw data. A single real number array holds the summed image for each minor frame.
- "Modified raw mode": Pixels below a selected threshold are set to zero, and pixels that are above that threshold are run-length encoded with x, y, and intensity information preserved.

*Analysis of diffraction data in the tactical time frame:* Immediately after a downlink of CheMin data, the downlink lead will process the minor frames to create 1-D 2q plots. These 1-D plots or "diffractograms" will be analyzed and compared with the ICDD (International Centre for Diffraction Data) PDF-2 powder diffraction file and the AMCSD (American Mineralogist Crystal Structure Database) to determine major mineral components. CheMin Science Team members will offer preliminary identifications of any major or clearly discernable mineral components during this tactical cycle. Periodically these data will support a "drive away" or "stay" decision for rover operations.

*Analysis and refinement of diffraction data in the strategic time frame.* Rietveld computational refinement methods and full pattern fitting, among others, will be utilized to perform a quantitative analysis of each pattern. These patterns will be compared with library patterns to identify mineral components and to derive quantitative mineral abundances. Analyses will be updated on a continuous basis as insights are made as to the identity of major and minor phases, and X-ray amorphous materials.

## MARS ON EARTH – UTILIZATION OF THE CHEMIN PROTOTYPE INSTRUMENTS DURING THE AMASE (ARCTIC MARS ANALOG SVALBARD EXPEDITIONS) TO SVALBARD, NORWAY

The first deployment of CheMin IV to Svalbard was thought provoking for us, because while we had approached it principally as a technology demonstration, we discovered quickly that *in situ* mineralogical analyses were actually useful for the geologists conducting fieldwork. The change from the usual procedure of first conducting field work and later performing laboratory mineralogical analysis suffers for the fact that hypotheses generated in the field can typically only be evaluated after the

geologists have left the field area. Geologists commonly collect a comprehensive set of samples from the field and make the assumption that the mineralogical information necessary to support or modify an already formed hypothesis is in hand. With *in situ* mineralogical analyses, field geologists are able to test hypotheses while in the field, and alter their collection/analysis strategy (or even modify their working hypotheses) based on the field data. However, in order for CheMin IV to be truly useful, user-friendliness, portability and pattern acquisition speed had to be improved. The next generation system was called mini-CheMin, and was made smaller and more portable, and contained all the hardware and software necessary to provide diffractograms as data were collected (Fig. 8). Diffraction data are transmitted wirelessly to a laptop system and analyzed using commercial programs like MDI™ Jade or Xpowder™. MiniCheMin proved to be highly useful, and a commercial version called "Terra" is now offered by a company called inXitu, Inc. With increased tube power and optimized geometry, XRD patterns of complex mineralogies can be acquired in 5-15 minutes, and single minerals such as quartz can be identified in as little as 20 seconds. With the increase in data collection speed, field-deployed XRD is now possible on the same time scale as other field-portable techniques such as XRF Spectrometry, laser-Raman and IR imaging. The advantage of XRD over these other techniques is that it is a true phase identification technique, and it is possible to quantify mineralogical results.

When a rover is deployed on Mars, time is money. If one divides the full cost of a Mars rover by the number of sols (days) in its active mission, the result is typically millions of dollars per sol. Decisions to move the rover, collect a sample or deploy one instrument vs. another are made on a time-critical, tactical basis. Because data are relayed to an orbiting Mars satellite only when the rover is in sight of the orbiter, then downlinked to the Deep Space Network (DSN) on Earth only when the orbiter is in sight of Earth, just a few hours are available for the Science Operations Working Group (SOWG) to analyze the data before the next command sequence has to be uplinked to the rover. During this time, the SOWG must converge on an interpretation of the downlinked data, come to a consensus as to the next day's operations, then code and relay those instructions through the DSN to the Mars orbiting satellite and down to the rover. Each day's activities are proscribed by the total energy and time made available to the instrument suite, the energy and time required for data acquisition for each individual instrument, the priority of desired measurements, and the total data volume that can be transmitted back to Earth. All of this means that instrument deployment and data interpretation, as well as the sequence in which particular measurements are made, require a thorough knowledge of instrumental capabilities, limitations and instrument synergisms one to another.

**Figure 8.** Use of Terra during NASA and other field campaigns. (a) The author (NASA/ARC) during the Scarab/RESOLVE field test on Mauna Kea, HI (2008). Terra was used to analyze as-received volcanic soils and partial run products from In Situ Resource Utilization (ISRU) experiments. Lunar oxygen-generating equipment in the background. (b) Doug Ming (NASA/JSC) on an expedition to the dry valleys of Antarctica (2008). Terra was used to analyze soils and other materials to understand pedogenesis (soil generation) in cold, dry climates. (c) Ron Peterson (Canadian Geological Survey), in the high Arctic of Canada (2009). Searching for low-temperature stability minerals such as the hydrates of iron and magnesium sulfate. (d) The author (NASA/ARC) during the AMASE expedition in Svalbard, Norway (2009). Analyzing carbonate sediments and cements in volcanic vents for clues as to their origin.

Many instrument providers have not had

prior experience in instrument operations on Mars (the author included). So that potential instrument providers can become proficient in these activities, NASA initiated a program called the Astrobiology Science and Technology for Exploring Planets (ASTEP). Typically, ASTEP deployments involve instrument operations in remote areas of Earth, on Mars-like (or other extraterrestrial) terrains. Two types of activities are conducted: In one type of activity, a scientific theme is pursued that has relevance to future missions: Habitability, Life Detection or Sample Return among them. A variety of instruments is utilized in the field to collect data useful in solving the multidisciplinary science or engineering problem that is posed. In a second type of activity, called a "Fast-Motion" field test ("FMFT"), a suite of Mars analog instruments is deployed in the field by one group of scientists ("the rover team") while a second group of scientists (the Science Operations Working Group, or "SOWG") is sequestered away from the field area. The SOWG learns about the field area by deploying "rover instruments" and analyzing data returned by the rover team under the same constraints that are faced by a SOWG during a real Mars mission (except that several Mars sols of activity can be completed in a single day).

Svalbard, Norway is an ideal location for ASTEP instrument deployments. At nearly 80° North latitude, the archipelago is almost devoid of plants larger than mosses, and mountain glaciers have created deeply scoured valleys, effectively the world's largest "road cuts" (Fig. 9). Rock exposures are breathtaking, and the lack of human habitation (with the exception of a few isolated towns) has left much of the landscape pristine. Svalbard has official status as an International Science Preserve, managed by the Norwegian government.

Initial interest in Svalbard for NASA research activities was engendered by the petrologic field work of Hans Amundsen (then at the University of Oslo).[6] In 1997-1999, in the midst of the flurry of research activities associated with characterizing the ALH84001 meteorite (which was purported to have evidence of life[7]), Amundsen collaborated with Allan Treiman of the Lunar and Planetary Institute and the author (Ames Research Center) to characterize carbonate globules similar to those described from ALH84001, found in ultramafic xenoliths from Svalbard.[8] Now in its 7th year, AMASE conducts yearly expeditions to Svalbard, providing a base of operations for scientists and technologists from many countries. Both NASA and ESA (European Space Agency) use AMASE as a testing ground for flight instrument prototypes and for conducting interdisciplinary science similar to that which occurs during landed planetary missions.

There is a variety of sedimentary, metamorphic and volcanic terrains in Svalbard.[9] CheMin prototype instruments such as Terra have principally been deployed in volcanic areas, analyzing basalts, volcanic soils,[10] ultramafic xenoliths and their weathering products[11] and secondary Fe-Mg carbonates associated with late-stage hydrothermal events.[12] Hydrothermal activity associated with volcanism was probably common on early Mars, which featured abundant basaltic rocks, water as ice or liquid, and heat from volcanoes and asteroid impacts. The most primitive forms of life on Earth still prefer hydrothermal environments, and such environments – and their habitability - can be studied either as presently active systems, or as fossil systems in the geologically near-recent of Svalbard. Early organisms were probably chemolithotrophic (they derived their energy from inorganic reactions in rocks), and a second possible habitable zone for early chemolithotrophic organisms in Svalbard is created by the weathering of ultramafic minerals such as olivine to form serpentine with the release of hydrogen.[13]

The style of volcanism in Svalbard is unique, in that the eruptive activity apparently occurred under ice, and the source magmas were volatile rich. Ultramafic xenoliths comprise as much as 20% of the volume of eruptive material, suggesting a deep source for the magma. Several Quaternary volcanic centers are prominent in the field areas studied by AMASE. Sverrefjell is a stratovolcano or large cinder cone ~500 m tall on the shore of Bokfjord (Fig.

9). Horizons of pillow lavas, indicative of eruption in water or under ice, exist nearly to the top of the volcano, and glacial erratics can be found at Sverrefjell's summit, indicating that the volcano was covered with thick ice either during or soon after its eruption. The style of eruption of Siggurdfjell is less obvious but probably was a volcanic neck or fissure, exposed up to 1000 m above present sea level. Fe-Mg carbonates are found in a variety of petrologic rock types and regimes on both Sverrefjell and Siggurdfjell. Ultramafic xenoliths, abundant at both localities, contain carbonate globules nearly identical to those found in ALH84001.[8] Several styles of volcanic vents, 1-10 m in width (Fig. 10) contain films, rinds or thick crusts of carbonate material, clearly precipitated from water in localized hydrothermal systems during the waning stages of eruptive activity. The Terra instrument was used for *in situ* analysis of these carbonates both at the sites of deposition, and aboard the Research Vessel Lance (our field station) directly after collection. These on-site mineralogical analyses allowed the formulation of hypotheses and collection/analysis strategies while scientists were still in the field, and also were used to direct the collection of samples used for other purposes, such as life marker chip, IR, laser Raman, Laser-Induced Breakdown Spectroscopy (LIBS) and Gas Chromatography-Mass Spectrometry (GC-MS).[14]

The value of Svalbard as a Mars analog site was recently proved out in a paper identifying carbonate-rich outcrops on Mars from data obtained during operations of the MER rover *Spirit*.[15] In the paper, the authors reported finding carbonates with nearly identical composition to the ALH84001 meteorite and to those reported from Svalbard[11] and concluded that the Martian carbonates were formed in basaltic hydrothermal systems, analogous to those described from Svalbard.

Less obvious but equally valuable are the personal bonds formed by the various interactions, arguments, compromises and group decisions made by geologists, biologists, chemists, physicists and engineers during many days of joint field activity and Fast Motion Field Tests. Interdisciplinary cooperation in the field between different scientific specialties, as well as between scientists of different nationalities, is also a hallmark of joint expeditions such as AMASE. As a result of the common interests of NASA and ESA, and the high cost of "going it alone" when it comes to planetary exploration, a decision was recently reached by these agencies

**Figure 9.** Sverrefjell Volcano, Svalbard, Norway. Sverrefjell was apparently erupted under a thick ice sheet and later bisected by a km-thick glacier. Pillow lavas indicative of eruption at sea level or below are evident at several levels on the cindercone, and glacial eratics can be seen at all levels, including at the summit.

**Figure 10.** Volcanic vent. One wall of a breccia-filled vent showing carbonate cementation (orange) of the basaltic breccia. In all likelihood, original volcanic vents such as this one acted as a plumbing system for late stage hydrothermal systems under the ice. Large Norwegian (Hans Amundsen) shown for scale.

to work together on future Mars exploration. The collaboration, cooperation and respect engendered by joint research endeavors on Earth such as AMASE will pay dividends when the real missions come to fruition.

## FUTURE VERSIONS OF CHEMIN FOR MARS AND OTHER SOLAR SYSTEM DESTINATIONS

A major drawback of CheMin XRD/XRF instruments developed to date is that samples must be prepared and delivered to the instrument as fine-grained powder. Two next-generation CheMin-like instruments funded for development by NASA are intended to minimize or overcome these sample handling problems. Luna (Fig. 11) is an XRD/XRF instrument intended for robotic missions to the Moon or any other airless body. Luna is a reflection mode instrument that will analyze soils without sample preparation. While there is still a requirement for fine-grained samples (as there is for all *powder* XRD instruments), the reflection geometry allows for less sophisticated sample delivery and sample handling systems. Due to the geometrical considerations of a compact reflection instrument, the low 2q limit is 8° 2q, too high for the detection of some clays. However, for almost all other minerals of geological interest, the lowest 2q peaks of interest are not lower than 15° 2q. A second Hybrid single crystal / powder XRD instrument is being designed and built as an arm instrument for small rovers (Fig. 12).[16] No sample preparation will be necessary for this instrument, except perhaps for the creation of a flat surface much as the Rotary Abrasion Tool (RAT) creates on the *Spirit* and *Opportunity* rovers. As-received powders such as soils can be analyzed via powder XRD, much like Luna, but with multiple detectors (and multiple wavelengths of radiation). Rocks with mineral grain sizes larger than fine-grained powder (most crystalline rocks would fall into this category) would be analyzed using the single crystal Laue technique. This capability is made possible through the use of multiple energy-discriminating area detectors. Single crystal

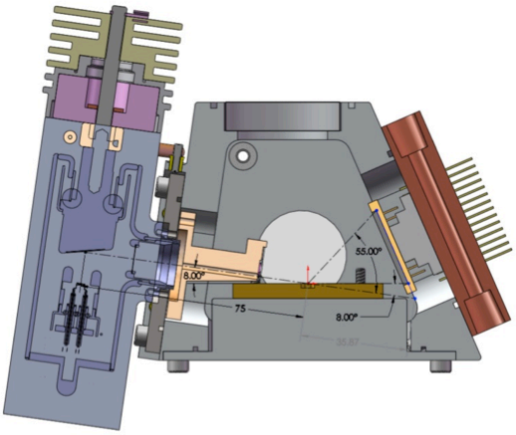


**Figure 11a**. Cross sectional diagram of the proposed LUNA instrument.

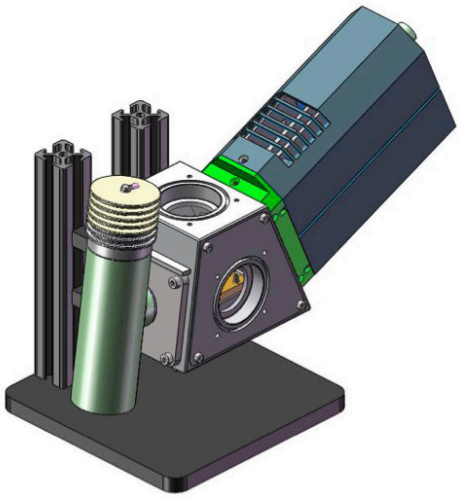

**Figure 11b.** Solidworks model of the prototype instrument as it will be built.

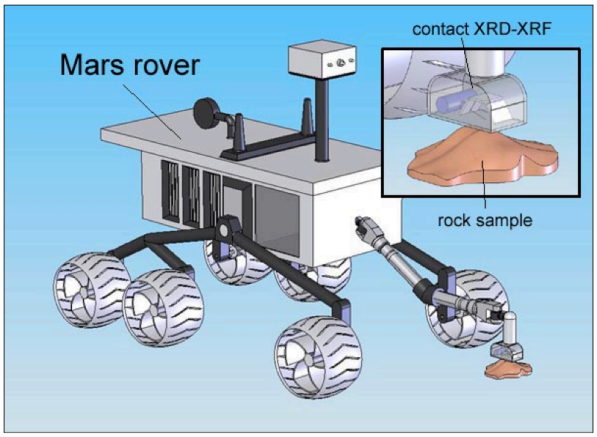


**Figure 12a.** Implementation of a hybrid – XRD/XRF on a rover arm.

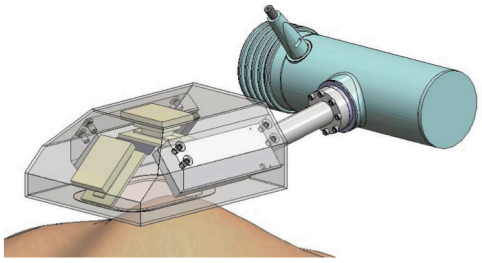

**Figure 12b.** Layout of the critical components of the system. From right to left: X-ray tube, collimator, sensor head.

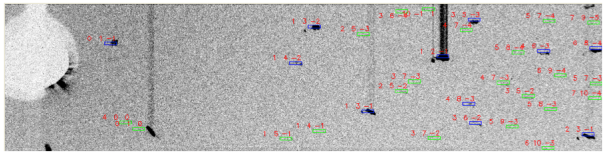

**Figure 12c.** Laue image of olivine marked with Miller indices found by the analytical software. Vertical lines result from the spreading of X-ray signal during CCD readout in positions of intense diffraction.

maxima can be identified by their energy and 3-dimensional position in space, and related back to the structure (and therefore identity) of the diffracting mineral phase.

## SPINOFF CHEMIN INSTRUMENTS FOR TERRESTRIAL USE

Several instruments based on the CheMin design are now in commercial production. Terra is used as a CheMin analog instrument in NASA-sponsored field campaigns as well as a number of ESA and other field expeditions throughout the world. Terra is also used for mud-logging applications at oil drilling sites, in museums and at remote sites for analyzing geological materials for industrial processes.[17]

Pharmaceutical products are typically crystalline, and can be identified and quantified by XRD just as minerals are. The author is working with scientists from the Centers for Disease Control (CDC) and elsewhere to develop applications of Terra for the identification of counterfeit drugs in developing nations. First and foremost of these are the Malaria drugs. Nearly 1.5 million people, mostly children in developing nations, die of Malaria each year.[18] Tens of thousands of these deaths are due to the scourge of counterfeit drugs, which in some places in SE Asia and equatorial Africa account for more than 50% of the drugs available.[19] Simple and effective tests have been devised to detect the presence or absence of the active ingredient in malaria pills, artesunate. However, an increasing number of these counterfeit malaria drugs are being "salted" with a small amount of artesunate to escape detection by these tests. This unfortunate practice is creating resistance in the malaria parasite for what is now the only drug that is effective in fighting the worst strains of the disease.[20] Terra is quite good at quantifying artesunate in malaria pills and can do so in remote locations, at the source of the problem.[21]

CheMin-type instruments are also being used in the world of Art and Antiquities. A reflection XRD instrument called "Duetto" was commissioned by Giacomo Chiari of the Getty Conservation Institute for characterizing art objects and intiquities.[17,22] This instrument is now being used world-wide to characterize sensitive archeological artifacts, to evaluate the causes of deteriorization of ancient murals and other artifacts in places such as Tutankhamen's tomb and the Roman ruins of Herculaneum, Italy (Fig. 13).

**Figure 13.** Duetto Instrument with Mummy. Duetto, commissioned by the Getty Conservation Institute, is a commercial spinoff of CheMin, is used for *in situ* art characterization and art conservation.

## FOOTNOTES

1. http://msl-scicorner.jpl.nasa.gov/Instruments/.
2. Bish, D.L. and J.E. Post (1993). "Quantitative mineralogical analysis using the Rietveld full-pattern fitting method." American Mineralogist 78, 932-942.
3. Chipera, S.J. and D.L. Bish (2002). "FULLPAT: a full-pattern quantitative analysis program for X-ray powder diffraction using measured and calculated patterns." J. Applied Crystallography 35, 744-749.
4. Bish, D.L., Blake, D., Sarrazin, P., Treiman, A.H., Hoehler, T., Hausrath, E.M., Midtkandal, I., and Steele, A. (2007). "Field XRD/XRF mineral analysis by the MSL CheMin instrument." LPSC XXXVIII, Abstract #1163.
5. Sarrazin, P., W. Brunner, D. Blake, M. Gailhanou, D.L. Bish, D. Vaniman, S. Chipera, D.W. Ming, A. Steele, I. Midtkandal, H.E.F. Amundsen and R. Peterson (2008). "Field studies of Mars analog materials using a portable XRD/XRF instrument." LPSC XXXIX, Abstract #2421.
6. Amundsen, H. E. F. (1987). "Evidence for liquid immiscibility in the upper mantle." Nature, 327, 692-695.
7. McKay, D.S., E.K Gibson Jr., K.L. Thomas-Keptra, H. Vali, C.S. Romanek, S.J. Clemett, X. D.F. Chillier, C.R. Maechling and R.N. Zare (1996). "Search for Past Life on Mars: Possible Relic Biogenic Activity in Martian Meteorite ALH84001." Science 273, 924-930.
8. Treiman, A.H., H.E.F. Amundsen, David F. Blake and Ted Bunch (2002). "Hydrothermal origin for carbonate globules in Martian meteorite ALH84001: a terrestrial analogue from Spitsbergen (Norway). EPSL 204 (2002), 323-332.
9. Harland, W.B. (1997). "The Geology of Svalbard." Memoir 17, Geological Society of London (521 p.).
10. Hausrath, E.M., Treiman, A., Bish, D.L., Blake, D., Sarrazin, P., Vincenzi, E., Midtkandl, I., Steele, A., and Brantley, S.L. (2009). "Short and long-term olivine weathering in Svalbard, and implications for Mars." Astrobiology 8(6), 1061-1069.
11. Treiman, A.H., K.L. Robinson, D.F. Blake and D. Bish (2010). "Mineralogy Determinations by CheMin XRD, Tested on Ultramafic Rocks (Mantle Xenoliths)." AbSciCon 2010, Abstract #5351.
12. Blake, D.F., H.E.F. Amundsen, L. Benning, D. Bish, P. Conrad, M. Fogel, I. Midtkandal, D. Ming, A. Steele, A.H. Treiman and the AMASE team (2010). "Carbonate cements from the Sverrefjell and Sigurdfjell volcanoes, Svalbard Norway; Terrestrial analogs for Martian carbonates?" AbSciCon 2010, Abstract #5119.
13. Schulte, M., D. Blake, T. Hoehler and T. McCollom (2006). "Serpentinization and its implications for life on the early Earth and Mars." J. Astrobiology 6(2), 364-376.
14. Steele, A., H.E.F. Amundsen, P.G. Conrad, L. Benning and the AMASE '09 Team (2010). "Arctic Mars Analogue Svalbard Expedition (AMASE) 2009." AbSciCon 2010, Abstract #5674.
15. Morris, R.V. et al (2010). "Identification of Carbonate-Rich Outcrops on Mars by the Spirit Rover." Sciencexpress, / www.sciencexpress.org / 3 June 2010 / Page 1-8 / 10.1126 / science / 1189667.
16. Sarrazin, P., P. Dera, R.T. Downs, D. Blake, D. Bish and M. Gailahou (2009). "Hybrid X-ray Diffraction for Planetary Mineralogical Analysis of Unprepared Samples." LPSC XXXX, Abstract #1496.
17. Wilkinson, M. (2010). "Beyond Terra Firma." Chemistry World, March 2010 pp. 50-53 (www.chemistryworld.org).
18. Marshall, A. (2009). "The Fatal Consequences of Counterfeit Drugs." Smithsonian Magazine, Oct. 2009; Finkle, M., (2007). "Malaria: Stopping a Global Killer." National Geographic, July, 2007.
19. Newton, P.N. et al (2008). "A Collaborative Epidemiological Investigation into the Criminal Fake Artesunate Trade in South East Asia." PLoS Medicine l www.plosmedicine.org, February 2008, Vol. 5, Issue 2, pp. 209-219.
20. Newton, P. N. et al (2006). "Manslaughter by Fake Aretesunate in Asia – Will Africa Be Next? Plos Medeine 3(6):e197. DOI:10.1371 / Journal.pmed.0030197.
21. Blake, D.F., Philippe Sarrazin, Bradley W. Boyer and Tyler C. Jennison (2010). "The use of field-portable p-XRD for the rapid identification of counterfeit pharmaceutical products and subsequent excipient identification and quantification." PPXRD IX, Abstracts w/program, Hilton Head Island, SC.
22. http://www.inxitu.com/new/html/duetto.html, http://www.inxitu.com/images/Duettowhitepaper.pdf
23. Chiari, G. (2009) "Saving Art in situ." Nature Vol. 453, 159.
24. The author is grateful for nearly 20 years of support from NASA-sponsored research and SBIR activities that made this instrument possible. Thanks also to the many dedicated engineers, technicians, scientists and managers at the Jet Propulsion Laboratory, Pasadena, CA who made the CheMin FM a reality.

## APPENDICES

*APPX. A.* The CCD imager is operated in single photon counting mode (the CCD is exposed and read often enough so that in the vast majority of cases, pixels contain either background noise or the charge from a single photon). When a single X-ray photon is absorbed in a single pixel of the CCD, the energy of the photon is dissipated in the volume of the pixel as electron-hole pairs. Each electron-hole pair has about 3.65 eV of charge associated with it. The energies of X-ray photons from elements of geological interest range from a few hundred to many thousands of electron volts. A calcium Ka x-ray fluoresced from the sample, for example, has an energy of 3.68 KeV, and would create slightly more than 1,000 electron hole pairs in the CCD. A cobalt Ka photon from the X-ray source that has an energy of 6.99 KeV, would produce 1,917 electron hole pairs in the sample.

*APPX. B.* A maximum of 65 $mm^3$ of sample material is delivered to the piezoelectrically vibrated funnel system that penetrates through the rover deck (during the time period when CheMin is not receiving samples, the CheMin inlet is protected by a cover). The funnel contains a 1 mm mesh screen to keep larger than expected grains from entering the CheMin sample handling system. Grains that cannot pass through the screen will remain there for the duration of the mission (samples will have been prescreened first to <1.0 mm and then to <150 µms in the CHIMRA sorting chamber, to prevent clogging of the CheMin funnel screen). Any grains <1.0 mm and >150 µm that pass through the screen will pass into the upper reservoir portion of the sample cell, where they will remain until the cell is inverted and they are dumped into the sump. However, under nominal conditions, the funnel will only receive material that has passed through the CHIMRA's 150 µm sieve. For the lifetime of the mission, CheMin is required to accept and analyze material delivered from CHIMRA with no more than 5% internal contamination between samples. Self-generated contamination originates from material that has remained in the funnel from previously delivered samples (and co-mingled with subsequent samples), or from material that has remained in previously used analysis cells (each cell will be used two to three times to accommodate 74 analyses during the nominal mission). CheMin empties used sample cells by inverting and vibrating the cell into a sump inside the instrument. Contamination is reduced by sample dilution; aliquots of sample material can either be dumped into the funnel and delivered directly to the sump through a shunt in the wheel without entering a sample cell (to remove funnel contamination), or a previously used sample cell can be filled with an aliquot of sample material, shaken and emptied to the sump prior to receiving a second aliquot of sample for analysis (to remove sample cell contamination). This processes requires coordination with CHIMRA to deliver more than one aliquot of a given sample.

*APPX. C.* The collimated ~50 µm diameter X-ray beam illuminates the center of an 8 mm diameter, 175-µm thick sample cell bounded by 6 µm thick Mylar or Kapton windows. The sample introduced into the funnel consists of <65 $mm^3$ of powdered material with a grain size of <150 µms. Only about 10 $mm^3$ of material is required to fill the sample cell. The remaining sample material occupies a reservoir above the cell. As a sample cell is filled, analyzed and dumped, it is shaken by a piezoelectric actuator (piezo). The piezo is driven at the resonant frequency of the sample cell assembly, which creates bulk convective movement of the sample similar to a liquid, delivering sample grains in random orientation into the volume irradiated by the beam. A nominal resonant frequency of 2150 Hz is characteristic of the tuning forks designed for CheMin.

During the moderate shaking which results in grain convection, it is possible that phase segregation will occur as a result of size or density differences between individual mineral grains. To reduce this problem CheMin can episodically use larger shaking amplitudes (we call this "chaos mode") to homogenize particle size or density segregations in the sample chamber.

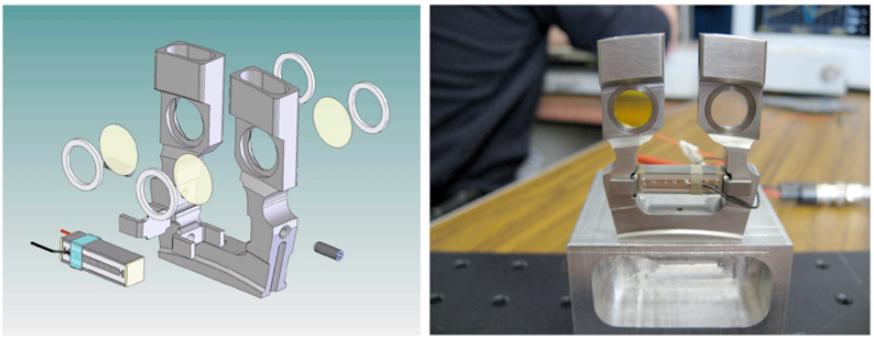

**Figure 5.** CheMin sample cells: (left), exploded view of dual-sample cell. Each dual-sample cell is a tuning fork driven at resonant frequency by a piezoelectric stack. The amplitude of shaking can be changed as a function of input voltage to the piezo. Each cell is an 8mm diameter X 170 $\mu$m thick volume bounded by X-ray transparent plastic films. During analysis, the piezo stack vibrates the cell at resonance, creating a turbulent flow of grains in the cell. Over time a myriad of grains from the sample flow past the 50 $\mu$m X-ray beam in random orientations. A reservoir above each sample cell holds excess material. The dual-cell assemblies are machined from solid titanium, and have a reproducible positioning accuracy (sample-to-detector path length) of less than 10 microns, 1/10$^{th}$ the diameter of a human hair).

The CheMin sample cells are constructed in dual-cell "tuning-fork" assemblies with a single horizontally driven piezoelectric actuator in each assembly (Fig. 5). Sixteen of the dual-cell assemblies are mounted around the circumference of the sample wheel. Five of the cells will be devoted to carrying standards; the other 27 cells are available for sample analysis and may be reused by dumping samples into the sump after analysis (Fig. 4).

Both Mylar and Kapton window cells are mounted on the wheel. Each window type has both benefits and drawbacks, and the choice of window type will be made based on the nature of the sample that is being analyzed. Mylar windows have a very flat diffraction background but Mylar is less durable than Kapton under severe vibration and is susceptible to destruction if highly acidic samples (e.g., the iron sulfate hydrate mineral copiapite) are analyzed. Kapton windows are extremely durable under severe vibration and are not susceptible to acid attack, but have a small diffraction contribution at ~6-7° 2q (CoKa radiation) which could be mistaken for the (001) diffraction peak of some clay minerals. Windows of both Kapton (in 13 cells) and Mylar (in 14 cells) are used in the Flight Model (FM) and Development Model (DM), as shown in Fig. 4.

CheMin uses a 600x600 pixel E2V CCD-224 frame transfer imager operated with a 600x582 data collection area. The pixels in the array are 40x40 $\mu m^2$, with an active region of deep depleted silicon 50 µms thick. The front surface passivation layer is thinned over a substantial fraction of the active pixel area. The E2V CCD-224 imager is a modern version of the E2V CCD-22 that was specially built for an X-ray astronomy application. The large size of the individual pixels causes a greater percentage of X-ray photons to dissipate their charge inside a single pixel rather than splitting the charge between pixels. The enhanced deep depletion zone results in improved charge collection efficiency for high energy X-rays. The thin passivation layer makes the CCD sensitive to relatively low-energy X-rays (AlKa at 1.49 KeV, SiKa at 1.75 KeV).

In order to keep the CCD from being exposed to photons in the visible energy range (from X-ray induced optical fluorescence from the sample) during analysis, a 150 nm Al film supported on a ~200 nm polyimide film is suspended in front of the detector. The detector itself is cooled to ~-60 °C by a cryocooler. The actual temperature of the CCD depends on the temperature of the RAMP (Rover Avionics Mounting Platform) into which the cryocooler's thermal load is dissipated. By cooling the CCD, dark current is reduced, as well as the effects of damage to the silicon lattice caused by neutrons from the RTG and the DAN instrument.

# The ChemCam Instrument Suite on the Mars Science Laboratory Rover *Curiosity*: Remote Sensing by Laser-Induced Plasmas

**Roger C. WIENS[a], Sylvestre MAURICE[b], and the ChemCam team**
[a]Los Alamos National Laboratory, Los Alamos, NM 87545, USA
[b]Institute de Recherche en Astrophysique et Planetologie, Toulouse, France

When the Mars Science Laboratory (MSL) rover *Curiosity* lands on a phyllosilicate-rich Martian terrain in 2012, it will carry a number of new technologies for investigating the surface properties and environments. Almost every type of experiment is new to space flight, or at least new to Mars, except the imagers and the reliable Alpha Particle X-ray Spectrometer (APXS). New types of instruments include the first x-ray diffraction instrument, CheMin, and many aspects of the Sample Analysis on Mars (SAM) suite with its combined chemical processing capabilities, its multi column gas chromatograph mass spectrometer, and tunable laser spectrometer (TLS). Both SAM and CheMin have both been described in previous Geochemistry Newsletter articles (Mahaffy, 2009; Blake, 2010). Here we describe an equally novel instrument—ChemCam—intended for remote sensing in the vicinity of the rover.

Field rovers are generally equipped with instruments that can make measurements on a variety of timescales. Rapid measurements are needed to determine which samples are of greatest interest for those techniques that require longer time and more resources to analyze. The timescale for analysis must also take into account the spatial proximity. Instruments on the Mars Exploration Rovers (MER) and MSL fall into three categories: remote, contact, and in-situ. Remote analyses are typically rapid measurements of the surroundings that do not require time-intensive driving or positioning. Contact measurements require relatively little sample preparation, while in-situ instruments generally require the most time for not only positioning the rover to grab the sample, but also for grinding, sieving, and ingesting, taking several days in total for each analysis from decision-point to completion. One can consider sample selection as a funnel, with remote sensing carrying out the broadest sampling, contact instruments being selected for a narrower subset of samples, and the in-situ analyses being reserved for the samples of greatest interest. For the Pathfinder rover Sojourner, the only remote sensing tool was an imager. Ideally, however, remote sensing instrumentation can identify chemical and/or mineral compositions and preferably also identify critical parameters essential to understanding habitability and the biological potential for Mars, key goals for the MSL mission (Grotzinger, 2009).

The ChemCam instrument suite will fulfill MSL's need for rapid remote sensing by providing critical information as mentioned above and, at the same time, addressing additional issues raised by the MER investigations. Specifically, within the first year of MER operation two surface-related analytical issues emerged. One was the presence of weathering coatings on rocks on Mars (e.g., McSween et al. 2004; Haskin et al., 2005). How are these weathering layers produced? What could we learn if we had an instrument sensitive enough to carefully probe the weathering layers? Also, how did the weathering layers affect our interpretation of Martian rock compositions based on surface-level analytical techniques? A second issue was the ubiquitous presence of dust on rocks which interfered with traditional remote sensing techniques. If the rover had to drive up and brush off a sample in order to use its remote sensing technique, it should no longer be considered remote sensing.

It was into this context that we proposed laser-induced breakdown spectroscopy (LIBS) along with a context remote micro-imager (RMI) to provide compositional remote sensing for the MSL rover. In the LIBS technique a pulsed laser beam is focused to a small spot on a

| MSL Goal | ChemCam Investigation |
|---|---|
| Characterize geology of landing site | Rapid remote rock identification; quantitative elemental compositions |
| | Soil and pebble surveys, average soil composition, maturity, and exotic materials |
| | Detection and study of hydrated minerals |
| Investigate planetary processes of relevance to past habitability, including the role of water. | Rapid remote identification of surface ices |
| | Analysis for weathering coatings on rocks |
| | Study rock morphologies (RMI imaging) |
| | Analysis of samples that are inaccessible to the rover arm |
| | Assist arm and drill sampling |
| Assess biological potential of target environments | Remote identification of organic material |
| Investigate the presence of toxic materials | Check for abundances of Be, Pb, Cd, and As well above hazardous levels for humans |

**Table 1.** ChemCam investigation goals directly address MSL mission goals.

target, providing at least 10 MW/mm$^2$, sufficient energy density to ablate atoms and ions in electronically excited states, creating a localized, brief plasma. The plasma emits light for up to several microseconds as the species decay back to ground state. The light is collected and spectrally dispersed to observe the characteristic emission lines of the elements present in the sample. By calibrating the spectra against those of standards, elemental abundances are determined. LIBS has been under development for several decades (e.g., Cremers and Radziemski, 1987) as an outgrowth of spark spectroscopy, providing a chemical analysis tool for inhospitable environments. It is also related to inductively coupled plasma mass spectrometry (ICPMS). LIBS was initially used in-situ; however, the real advantage comes at close- and medium-range stand-off distances on natural targets (e.g., Wiens et al., 2002), in which case no sample preparation or handling is needed. As an active technique the laser pulses rapidly remove dust coatings and profile into solid surfaces, for example to study and to remove weathering layers, exposing the pristine rock. No other remote technique possesses these advantages.

The goals of the ChemCam investigation are listed in Table 1. These combine typical objectives of a remote sensing instrument, as discussed above, with specific capabilities of the LIBS investigation, especially where they align with major goals of the MSL mission. For example, unlike x-ray techniques, LIBS is sensitive to the light elements: H, Li, Be, B, C, N, and O. Importantly for Mars, it can identify H- or C-bearing materials and with proper calibration it can quantify the abundances of these elements. The complete ChemCam spectrum consists of 6144 channels covering three nearly overlapping spectral ranges from 240 to 850 nm. The spectrum is rich in emission lines, with many elements providing multiple emission lines. Overall, LIBS is sensitive to nearly all elements, but it is most sensitive to the alkali and alkali earth elements, with particularly low detection limits (e.g., < 100 ppm) for Li, Sr, and Ba. On the other hand, LIBS is relatively insensitive to elements on the other side of the periodic table, including S, Cl, and F. However, ChemCam can still detect sulfur at the several percent level, as expected for many materials on Mars.

It is thus fortuitous that *Curiosity* is equipped with both ChemCam and APXS, which is improved from the APXS units on the MER rovers. While ChemCam provides a large number of remote analyses, APXS, mounted on the rover arm, will provide a relatively smaller number of more accurate analyses. LIBS additionally provides very high spatial resolution (0.2-0.5 mm analysis spots) compared to APXS (~17 mm on MSL). ChemCam removes dust and weathering layers with multiple laser pulses,

while APXS on MSL will use a brush to remove dust. And finally, while ChemCam is sensitive to light elements and is highly sensitive to alkalis, APXS will have significantly better sensitivity for sulfur and halogens. As can be easily seen, these capabilities are highly complementary.

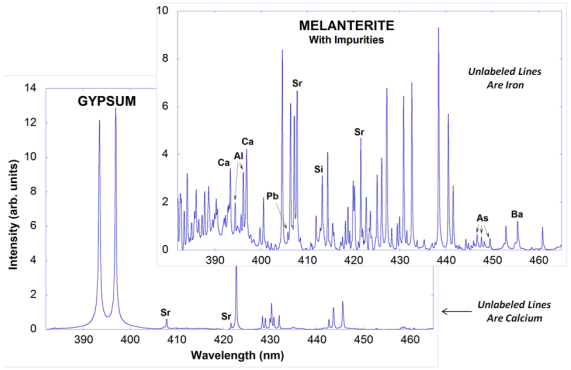


**Figure 1.** A portion of the ChemCam LIBS spectrum (one third of its channels) contrasting a relatively pure gypsum sample and an impure melanterite, both analyzed at 3 meters distance. Emission lines from S, O, and H (not shown here) are recorded by the longer wavelength spectrometer.

Fig. 1 shows two contrasting LIBS spectra of rock powder standards recorded at 3 m distance with one of ChemCam's three spectrometers, using about two thirds of the full laser energy (10 vs. 15 mJ). In the spectrum of the relatively pure Gypsum sample ($CaSO_4 \cdot 2(H_2O)$; $[SiO_2] = 0.45\%$ in this sample) all of the visible emission lines in this range are due to Ca except the two labeled Sr lines (930 ppm). The emission lines of H, O, and S are visible in other spectral ranges covered by ChemCam. By contrast, the spectrum of a quite impure melanterite ($FeSO_4 \cdot 7(H_2O)$ in pure form; the low magnitude of the 656 nm H peak suggests it converted to szmolnokite, the monohydrate form, in the Mars chamber) shows a plethora of emission lines, most of which are due to iron (all unlabeled peaks in the figure). However, the emission lines from a number of impurities can be seen, including Si ($[SiO_2] = 68\%$), Ca ($[CaO] = 0.1\%$), Al ($[Al_2O_3] = 0.9\%$), Sr (1930 ppm), As (960 ppm), Ba (450 ppm), and Pb (300 ppm; listed abundances are based on literature values). In general, transition elements such as Fe, Mn, Cr, V, and Ti display large numbers of LIBS emission lines, as seen in the case of Fe in the melanterite spectrum, while a smooth baseline, such as seen in the gypsum spectrum in Fig. 1, is only found in samples lacking transition elements.

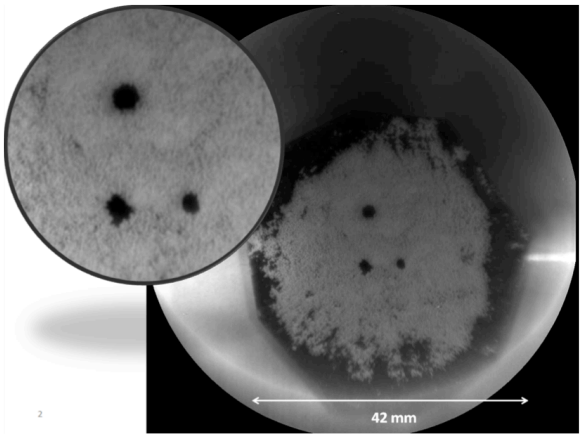


**Figure 2.** ChemCam Remote Micro-Imager (RMI) image showing laser removal of dust from a smooth rock surface at a distance of 2.9 m from the instrument. The sample was in a 900 Pa atmosphere, simulating the Mars environment.

The ability to remotely remove dust using the laser is shown in an image taken by ChemCam's RMI imager in Fig. 2. The white dolomite powder (> 70% of the material has grain size < 20 µm) shown in this figure was screened off at a uniform height of 25 microns above the surface of a smooth slab of basalt. The three LIBS analysis spots were produced at 2.9 m distance with lower laser energies (7.5 mJ, right, and 10 mJ for the two on the left) than the 14 mJ to be used on Mars. Ten laser shots were used for the right and lower left spots, while 50 shots were used for the spot in the upper left. An enlarged view in the inset shows that the dust, which tended to clump together, was cleared from areas 1.5 to 2.4 mm in diameter. The actual analysis spots are smaller and are not seen without stretching the image contrast. Investigation of the individual spectra shows that in the case of the lowest energy laser analysis the composition effect of the dust was no longer seen in the spectrum by the fourth shot. A similar test was carried out with an inclined sample and a much thicker (>1 mm)

dust layer. The signature of the underlying rock appeared within the first ten laser shots. During the next several shots some of the dust fell back into the hole. By the time twenty-five pulses were fired the spectra were dust-free and remained that way as additional shots were sent. Depth profiles have been carried out in several homogeneous solid samples of carbonate and basalt. For analyses of up to 1000 pulses, depths in the range of 300-600 µm were achieved. More work is planned using layered rock targets with replica instrumentation understand how much contamination from the upper layer affects measurements of the lower layers (e.g., Cousin et al., 2011).

| | |
|---|---|
| Laser type | Nd: KGW |
| Laser pulse duration | 5 ns |
| Laser wavelength | 1067 nm |
| Laser repetition rate | 1-10 Hz |
| Laser pulse energy | 14 mJ |
| Laser spot diameter on target | 200-500 $\mu$m |
| LIBS nominal distance range | 1.5-7 m |
| Telescope aperture | 110 mm |
| Spectral range | 240-850 nm |
| Spectrometer type (3 units) | Cross Czerny-Turner |
| Spectral channels | 6144 x 14 bit |
| Spectral resolution (FWHM) | 0.2 nm (<500 nm), 0.65 nm (> 500 nm) |
| Spectral exposure | 10 ms – 10 s |
| RMI imager CCD | 1000 x 1000 pixels |
| RMI typical exposure, Mars | 40 ms |
| RMI imager resolution | 0.10 mrad |
| RMI imager field of view | 20 mrad |

**Table 2.** Key ChemCam instrument parameters

ChemCam's key parameters are given in Table 2. To facilitate rover accommodation, the instrument was built into two parts, as shown in Fig. 3. The laser, telescope, RMI, and associated electronics are located on the mast of the rover. The LIBS light collected by the telescope is transported to the spectrometers in the body of the rover via a 5.7 m long optical fiber. The physical division of the instrument facilitated construction by the two equal partners: The mast unit was constructed and tested under the leadership of the Institute de Recherche en Astrophysique et Planetologie (IRAP) at the Observatoire Midi-Pyrénées in collaboration with the Centre Nationale d'Etude Spatiale (CNES) in Toulouse, France. The body unit, including an optical demultiplexer, three spectrometers, electronics, data processing unit, and flight software, was constructed by Los Alamos National Laboratory (LANL). The instrument's software includes an autofocus routine and, for the RMI, an auto-exposure code. Jet Propulsion Laboratory characterized the CCDs, provided a thermo-electric cooler for the detectors, and developed the mast-to-body optical fiber in collaboration with Goddard Space Flight Center.

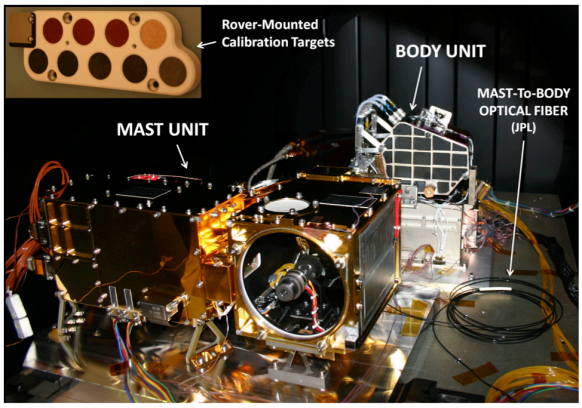


**Figure 3.** Components of the ChemCam instrument suite.

An on-board calibration target (Fig. 3) is installed on the rover at a distance of 1.54 m from the ChemCam telescope. The target consists of four igneous glasses, three of which were synthesized to replicate shergottite, picrite, and norite compositions, and one target is a natural macusanite glass (Fabre et al., 2011). The target also includes four ceramics fabricated from varying mixtures of Totavi basalt, gypsum, and either nontronite standard NAu-2 or kaolinite standard KGa-2 (Vaniman et al., 2009). Two additional materials in the target assembly are graphite to facilitate carbon quantification (Ollila et al., 2011) and titanium for wavelength calibrations and standardization.

ChemCam is designed and planned to be used daily on Mars. Operations planning divides the rover activities into reconnaissance sols (sol = Mars day), drive sols, approach sols, contact sols during which arm-mounted instruments APXS and MAHLI (hand lens imager) are used, and in-situ analysis sols during which CheMin

and SAM analyses are carried out. ChemCam can be used to perform reconnaissance on both of the first two types of sols. During approach sols ChemCam data will help select the precise sample for in-situ analysis, and during contact and in-situ analysis sols ChemCam can perform additional surveys of surrounding materials. A typical analysis will consist of a number of laser pulses sufficient to remove surface dust, followed by a number of laser pulses (e.g., 30) that will be averaged together for better statistics. At times depth profiles will be performed to understand the compositions of dust and weathering layers as well as the rock composition. Because the LIBS analysis spot size is by necessity ≤ 0.5 mm in diameter in order to achieve the energy density required to produce a plasma, determining a whole-rock composition requires multiple analysis spots for medium- and coarse-grained lithologies (Thompson et al., 2006; Anderson et al., 2011).

The instrument operation flow is shown in Fig. 4. Each analysis spot is expected to take about six minutes and two Watt-hrs, but in most cases it will be necessary to warm the laser from the -40°C survival temperature of the mast to its operation temperature of -10°C, taking about 20 minutes before the first analysis of the day. There is also some time required at the end of analyses to slowly cool the unit and to defocus to a sun-safe configuration and stow the mast. Of the actual analysis, the laser shots will normally operate at 3 Hz, taking only ~20 s, while up to 3 minutes is required for focusing and some tens of seconds are required for transferring the data. RMI context images will be taken before and after each LIBS analysis, transmitting only the pixels corresponding to the LIBS spot on the second image.

Consistent with the instrument itself, ChemCam's science team consists of French and US members in nearly equal representation. Operation of the instrument will also be shared. The length of Martian days being 39.6 minutes longer than Earth's, rover operations will precess relative to the terrestrial clock on a 36.4 day cycle. ChemCam operations will divide this into 18 days for French operation during the time in which the data come to Earth at an earlier time of day, and 18 days for US operations. Scientists from both countries will continually staff working groups tasked with rover planning, with the result that decision-making for ChemCam will not be completely run by one country at any time.

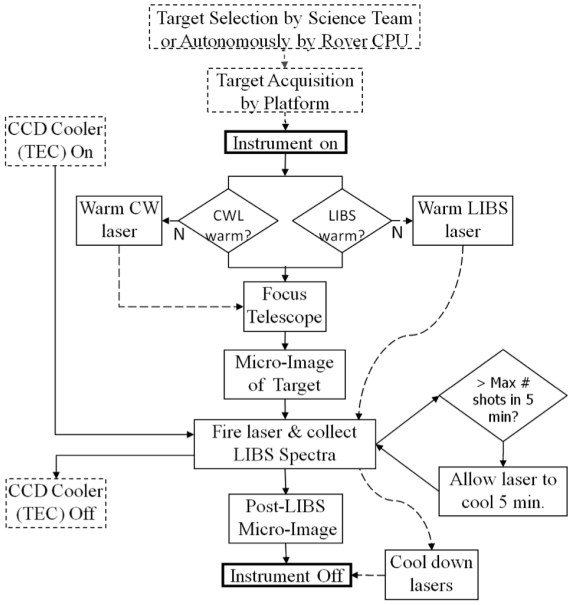


**Figure 4.** Operational flow chart for typical LIBS analysis. CWL = autofocus laser, TEC = thermo-electric cooler.

The LIBS data are rich in emission lines (Fig. 1), allowing the development of training sets of spectra of standards of known compositions, which are used with multivariate analysis techniques to perform: 1) rapid multivariate spectral classification to categorize samples by rock type, 2) multivariate analytical processing against a database of standards for quantitative elemental abundances, and 3) univariate analyses of individual emission lines in some cases. Data pre-processing begins with subtracting the non-laser-induced background from the active spectra, correcting for the instrument response and for wavelength drift, and identifying emission lines. For sample classification the team utilizes the linear projection algorithms of principal component analysis (PCA) and independent component analysis (ICA) (e.g., Comon, 1992; Sirven et al., 2007), complemented by the non-linear stretching technique of Sammon's map (Lasue

et al., 2011). Given the rapid daily turn-around needed for tactical data, these techniques will quickly inform the MSL team whether rocks or soil samples analyzed the previous sol are similar to or different from samples encountered previously on Mars.

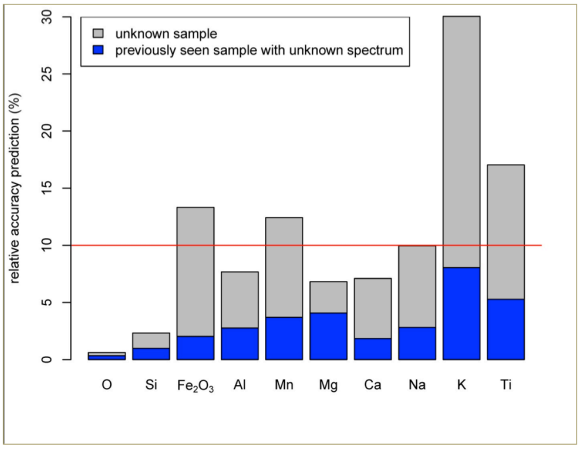


**Figure 5.** Median relative errors of predicted major element abundances for a set of basalt and andesite standards observed at 5 m distance with the ChemCam flight model (Wiens et al., 2011).

For quantitative analysis the team uses partial least squares (PLS) regression against agreed-upon sets of standards, the spectra of which are taken in terrestrial laboratories with replica instrumentation. Tests with data taken prior to instrument delivery show that analytical precisions and accuracies of the major elements generally meet the goal of ≤10% relative error. Median accuracies from two different PLS analyses of data taken at 5 m distance on ten basalt and andesite rock powder standards are shown in Fig. 5. Each analysis used fifty laser pulses and the spectra of all but the first five pulses were averaged together. Four spots were analyzed per sample. The figure shows that prediction accuracies are quite highly dependent on the quality of the match of standards to the unknown. The data shown in gray leave out all analyses of the unknown from the training set. By contrast, the blue bars show median errors obtained when three analysis spots of the same standard are included in the training set used to predict the fourth spot on a given sample. Although the composition of these three spots is identical to the unknown, this detail is not known by the algorithm. Even so, the accuracy is significantly improved, showing that matching the unknown closely with training set standards is important. As a result, in actual analyses an iterative approach must be taken in which a completely unknown sample is first estimated using standards covering a broad array of composition space to provide an approximate composition. The composition is further refined using a training set of standards focused to match the initially predicted composition. The ChemCam team plans to compare its Mars analyses against terrestrial standards analyzed in similar laboratory-based instruments to provide the needed training set for calibration.

Finally, in some cases univariate analyses of selected emission lines will be undertaken for specific studies. As an example, strontium displays only two relatively strong emission lines at 407.89 and 421.67 nm (cf. Fig. 2). For the on-board igneous calibration targets the latter Sr emission line produced an excellent calibration curve, as shown in Fig. 6.

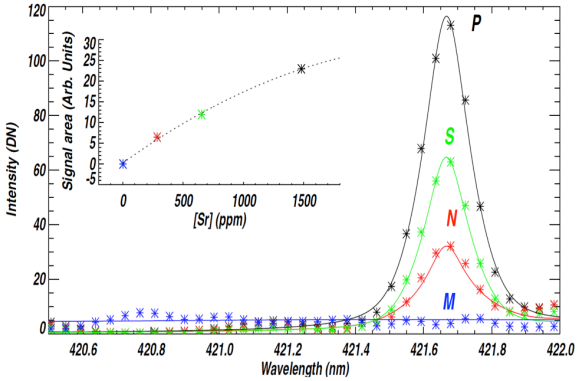


**Figure 6.** Emission line of strontium taken with ChemCam at 1.5 m distance showing the excellent detection limits for a trace element. Symbols indicate curves for macusanite (M), norite (N), shergottite (S), and picrite (P) synthetic compositions doped with Sr (Fabre et al., 2011)

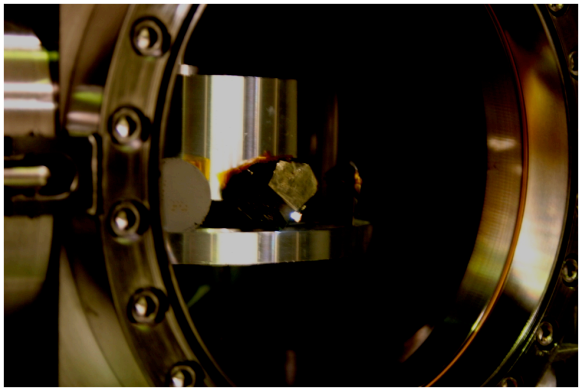

**Figure 7.** ChemCam emission spark erupts from a pyrite crystal in the LANL sample chamber at a distance of 8.7 m.

ChemCam will capture the public imagination as the first laser gun in space. Fig. 7 shows a ChemCam spark erupting from a pyrite crystal in air at 8.7 m distance. Iron- and sulfur-rich samples tend to couple to the 1067 nm laser beam better than ordinary rocks, so we were able to shoot this sample at a significantly longer distance than ChemCam's nominal limit of 7 m.

In summary, the ChemCam instrument suite includes the first LIBS experiment designed for space exploration. Its tactical role is to provide the MSL team with information on rocks and soils surrounding the rover, enabling efficient operations planning. It is a radical departure from previous remote sensing and the small spot analysis will be extremely useful in scanning across stratigraphic layers encountered by MSL. ChemCam's ability to study compositional variations among soil and rock layers provide for the first time a means to systematically investigate rock weathering and soil stratification. The ability to study light-element abundances directly addresses MSL and Mars goals to follow the water and to investigate habitability. These remote analyses are enabled by the removal of obscuring dust using the initial laser shots for cleaning the surface. ChemCam also provides the highest resolution context imaging of the analysis spots, enabling much better interpretation of the analyses than otherwise. Overall, ChemCam is a novel way to interrogate samples, effectively brushing and "ratting" (i.e., performing the same function as MER's rock grinder on) the analysis spot without needing the mechanical complexity of an arm touching the surface.

## ACKNOWLEDGEMENTS

A great many people on the ChemCam team and elsewhere are thanked for their contributions to this work. In particular, J. Lasue contributed the PLS plot, C. Dufour and R. Perez processed the RMI image, C. Fabre contributed the plot showing the Sr emission line detail. B. Barraclough, S. Clegg, S. Humphries, A. Ollila, R. McInroy, A. Mezzacappa, L.-M. Nortier, D. Delapp all worked to produce the ChemCam data, just to name a few. This work was graciously supported by CNES in France and by NASA's Mars Program Office through MSL in the US. The manuscript benefitted from comments by J. Lasue, P. Mahaffy, and two anonymous reviewers, and editorial support by S. Komor was greatly appreciated.

## REFERENCES

Anderson R.B., Morris R.V., Clegg S.M., Bell J.F.III, Wiens R.C., Humphries S.D., and Mertzman S.A. (2011) Remote quantitative chemical composition of rocks using laser induced breakdown spectroscopy with partial least squares and artificial neural network methods. Submitted to Icarus.

Blake D. (2010) A Historical Perspective of the Development of the CheMin Mineralogical Instrument for the Mars Science Laboratory (MSL '11) Mission. *Geochemical News 144*, September. http://www.geochemsoc.org/publications/geochemicalnews/gn144sep10/ahistoricalperspectiveofth.htm

Comon P. (1992),Independent component analysis, in: J.L. Lacoume, (Ed), Higher-Order Statistics, Elsevier, Amsterdam, 29-38.

Cousin A., Maurice S., Forni O., Wiens R., Berger G., and the ChemCam team (2011) Depth profiles studies using ChemCam. *Lunar Planet. Sci. LXII*. Abstract 1963. The Lunar and Planetary Institute, Houston, TX.

Cremers D.A. and Radziemski L.J. (1987) Laser plasmas for chemical analysis. Chapter 5 in *Laser-Induced Plasmas and Applications* (L.J. Radziemski, R.W. Solarz, and J.A. Paisner, eds.), Marcel Dekker, New York, pp. 351-415.

Fabre C., Maurice S., Cousin A., Wiens R.C., Forni O., Sautter V., and Guillaume D. (2011) Onboard calibration igneous targets for the Mars Science Laboratory Curiosity rover and the Chemistry Camera Laser Induced Breakdown Spectroscopy instrument. Spectrochim. Acta B, doi: 10.1016/j.sab.2011.03.012.

Grotzinger J. (2009) Beyond water on Mars. *Nature Geoscience* 2, 1-3.

Haskin L.A., and 29 co-authors (2005) Water alteration of rocks and soils on Mars at the Spirit rover site in Gusev crater. *Nature* 436, doi:10.1038/nature03640.

Lasue J., Wiens R.C., Forni O., Clegg S.M., Maurice S., Stepinski T., and the ChemCam team (2011) Non-linear mapping technique for data visualization and clustering assessment of LIBS data: Application to ChemCam data. J. Anal. Bioanal. Chem., DOI 10.1007/s00216-011-4747-3.

Mahaffy P. (2009) Sample Analysis at Mars: Developing analytical tools to search for a habitable environment on the red planet. *Geochemical News 141*, October. http://www.geochemsoc.org/publications/geochemicalnews/gn141oct09/sampleanalysisatmars.htm

McSween H.Y., and 34 co-authors (2004) Basaltic rocks analyzed by the Spirit rover in Gusev Crater. *Science* 305, 842.

Ollila A.M., Blank J.G., Wiens R.C., Lasue J., Newsom H.E., Clegg S.M., Cousin A., Maurice S. (2011) Preliminary results on the capabilities of the ChemCam laser-induced breakdown spectroscopy (LIBS) instrument to detect carbon on Mars. *Lunar Planet. Sci. XLII*. Abstract 2395. The Lunar and Planetary Institute, Houston, TX.

Sirven J.-B., Sallé B., Mauchien P., Lacour J.-L., Maurice S., and Manhes G. (2007) Feasibility study of rock identification at the surface of Mars by remote laser-induced breakdown spectroscopy and three chemometric methods. J. Anal. Atomic Spectrosc. 22, 1471-1480.

Thompson J., Wiens R.C., Clegg S., Barefield J., Vaniman D., and Newsom H. (2006) Remote LIBS Analyses of Zagami and DAG 476 Martian Meteorites. *J. Geophys. Res.*, 111, E05006, doi:10.1029/2005JE002578.

Vaniman D.T., Clegg S., Lanza N., Newsom H., Wiens R.C., and the ChemCam team (2009) Fabrication of sulfate-bearing ceramic calibration targets for the ChemCam laser spectroscopy instrument, Mars Science Laboratory. *Lunar Planet Sci. XL*. Abstract 2296. The Lunar and Planetary Institute, Houston, TX.

Wiens R.C., Seelos F.P. IV, Ferris M.J., Arvidson R.E., Cremers D.A., Blacic J.D., and Deal K. (2002) Combined remote mineralogical and elemental identification from rovers: Field and laboratory tests using reflectance and laser-induced breakdown spectroscopy. *J. Geophys. Res. Planets.*, 10.1029/2000JE001439, 30 August.

Wiens R.C., and 13 co-authors (2011) Calibration of the MSL / ChemCam / LIBS remote sensing composition instrument. *Lunar Planet. Sci. XLII*. Abstract 2370. The Lunar and Planetary Institute, Houston, TX.